ABSTRACT

NESTER, RYAN TIMOTHY. Organic Rankine Cycles: A Comparative Study and Analysis of Multiple Applications. (Under the direction of Dr. Stephen Terry).

An organic Rankine cycle (ORC) is a thermodynamic process that utilizes low temperature waste heat to boil a refrigerant causing it turn to vapor then forces that refrigerant through a turbine/generator combination in order to produce alternating current electricity. An ORC can be used in many applications to take heat that is otherwise wasted because it is vented to the atmosphere, and use it to produce electricity for the facility. This report is a case study of these applications and a brief analysis of the factors affecting the performance of the cycle. It was found that the solar thermal application of ORC's is an inapplicable option when using evacuated tube collectors and parabolic trough collectors. The working fluid for the ORC can be tailored to fit its applications, for instance R-123 should be used at lower pressures, whereas R-245ca should be used in high pressure/temperature applications, and R-245 is a great baseline fluid used for general applications. It was also found that most of the cycles operate at about 10% efficiency and can be increased by the use of a recuperator or by altering the operating condition based on the fluid selection. An economic analysis was also performed to look at the results of the simple payback period and costs of an ORC with escalating prices in electricity. It was found that the payback is greatly decreased as the price of electricity was increased. The mass flow rate of the waste heat input was also found to have a large impact on the amount of power an ORC can produce.

Organic Rankine Cycles: A Comparative Study and Analysis of Multiple Applications

by
Ryan Timothy Nester

A thesis submitted to the Graduate Faculty of
North Carolina State University
in partial fulfillment of the
requirements for the degree of
Master of Science

Mechanical Engineering

Raleigh, North Carolina

2011

APPROVED BY:

_____	_____
Dr. Tarek Echekki	Dr. Herbert Eckerlin

_____
Dr. Stephen Terry
Committee Chair

DEDICATION

This thesis is dedicated to my parents because I never could have made it this far without their love and support. It is also dedicated to the rest of my family, friends, and loved ones. I think about you all daily.

BIOGRAPHY

Ryan Timothy Nester was born in Lakeland, Florida. He went to George W. Jenkins High School where he was introduced to Project Lead the Way, a program designed to introduce high school students to multiple disciplines of engineering. Project Lead the Way planted a seed in Ryan's head that would ultimately grow into the career in Mechanical Engineering that he has pursued over the past 6 years. Ryan studied Mechanical Engineering at Florida Institute of Technology then transferred to Florida State University where he received a Bachelor's degree in Mechanical Engineering with a specialization in Thermal Fluid Sciences and a minor in mathematics. Ryan then picked up his possessions in Florida packed a U-Haul and moved to North Carolina to attend North Carolina State University, where he received a Master's degree in Mechanical Engineering and studied energy efficiency. Ryan now resides in Maryland performing energy audits for Siemens building technologies division.

ACKNOWLEDGMENTS

I would like to acknowledge Dr. Stephen Terry for providing me with the opportunity to investigate manufacturing facilities and teaching me many ways to save energy and ultimately be more energy conscious. I would also like to acknowledge the great friends and future professional colleagues that I met at the IAC.

TABLE OF CONTENTS

LIST OF TABLES

LIST OF FIGURES

CHAPTER 1

1.1 Need

With the cost of energy constantly increasing and the whole world turning towards being more environmentally friendly and more energy efficient there is a need for more alternative and renewable sources of energy. One of these sources is an organic Rankine cycle (ORC). ORC's convert low temperature waste heat into electricity and emit absolutely no carbon dioxide or pollutants. ORC's fall under the category of micro turbines which mean that if a facility implements an ORC they are able to file for certain tax breaks and incentives from the state and federal government that can make the purchase and implementation of ORC's easier and cheaper for the facilities that are installing them. Although these cycles are only approximately 10% to 15% efficient they are utilizing energy from exhaust gases which is otherwise wasted and expelled into the atmosphere. Therefore they are essentially creating free energy and have the potential to save companies that install these cycles hundreds of thousands of dollars.

1.2 History

A Rankine cycle is the basic power production cycle used in about 80% of the electricity produced worldwide. The cycle is first accredited to, and named after, William John Macquorn Rankine a famous Scottish engineer and physicist. William Rankine first developed the, soon to be named, Rankine cycle after studying and developing the theory of heat engines in the early 1850's. The first publication of a Rankine cycle was in a published work by William Rankine in 1859. The basic Rankine cycle is a closed loop process that takes a working fluid and pumps the fluid through a boiler until it is changes phase and becomes a vapor, the vapor is then forced through a turbine which rotates a shaft that is connected to a generator that produces electricity, the vapor is then pushed through a condenser where the vapor is fully condensed to a liquid, the liquid then enters a pump and starts the cycle again. In the basic Rankine cycle the working fluid is water which is easily converted to steam in the boiler and can be used to produce electricity or can be used in a steam engine. The basic Rankine cycle setup and its temperature entropy curve can be seen in Figure 1.1.

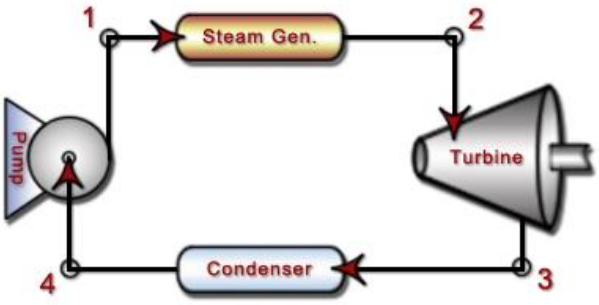

Figure 1.1a: Basic Rankine Cycle

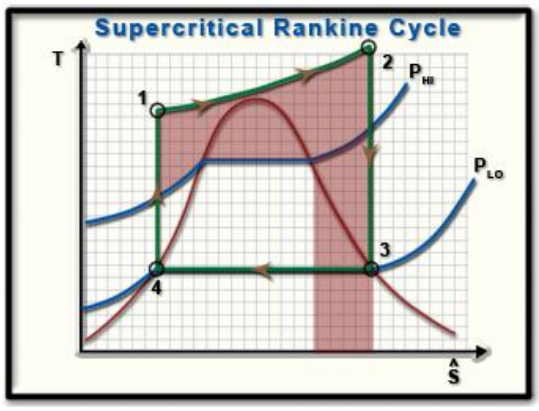

Figure 1.1b: Basic Rankine T-s Diagram

An organic Rankine cycle is a Rankine cycle that utilizes an organic based fluid as the working fluid. An organic fluid is defined as a fluid that contains carbon. The main types of organic fluids are refrigerants or hydrocarbon chain fluids. The first organic Rankine cycle was developed by two Israeli solar engineers, Harry Zvi Tabor and Lucien Bronicki. They originally started the Israeli Solar Engineering project in the late 1950's. They realized that low-grade heat was available from the sun and that they could convert this heat to electricity for use in rural areas that were unable to connect to the electrical grid directly.

They first looked at using a reciprocating engine but decided that there were too many moving parts and many maintenance issues for a very rural application so they decided to design the first organic Rankine cycle, which could utilize the low temperature waste heat and only had one moving part in the turbine. The first organic Rankine cycle was designed in 1961 and was displayed in the United Nations conference on New Sources of energy in Rome. The prototype was a three-kilowatt system and did not get widely produced after its premier.

In the 1970's and 1980's the organic Rankine cycle was looked at by many research groups, especially NASA and the Department of Energy (DOE), to be used in large prime movers, such as boats or trains, that are running for a long time and have a high exhaust rate. The main focus of these studies was to reroute the heat from the exhaust and use it in an organic Rankine cycle to provide electricity for the boat or train. Due to the lack of computer modeling and inability to produce efficient turbines at the time much of this research never

went anywhere, but now that more efficient systems and models are able to be produced, better organic Rankine cycles are commercially available.

1.3 Organic Rankine Cycle

An organic Rankine cycle is a basic power production cycle that utilizes low temperature waste heat to produce electricity. An organic Rankine cycle is similar to a Rankine cycle in the sense that it turns a fluid to a vapor and forces the vapor through a turbine which spins a shaft connected to a generator which in turn produces electricity. The vapor is then forced through a condenser that changes the vapor back to a liquid which then enters a pump and starts the cycle again. An organic Rankine cycle is different from a Rankine cycle because it uses a fluid that is organic based, meaning it contains carbon, and has a lower boiling point. Since the fluid has a lower boiling point the cycle can utilize lower temperature heat to cause the fluid to change phase from a liquid to a vapor. An example schematic of an organic Rankine cycle is shown below in Figure 1.2, this particular organic Rankine cycle incorporates a recuperator which takes the excess heat out of the fluid before it enters the condenser and uses it to preheat the fluid before it enters the evaporator.

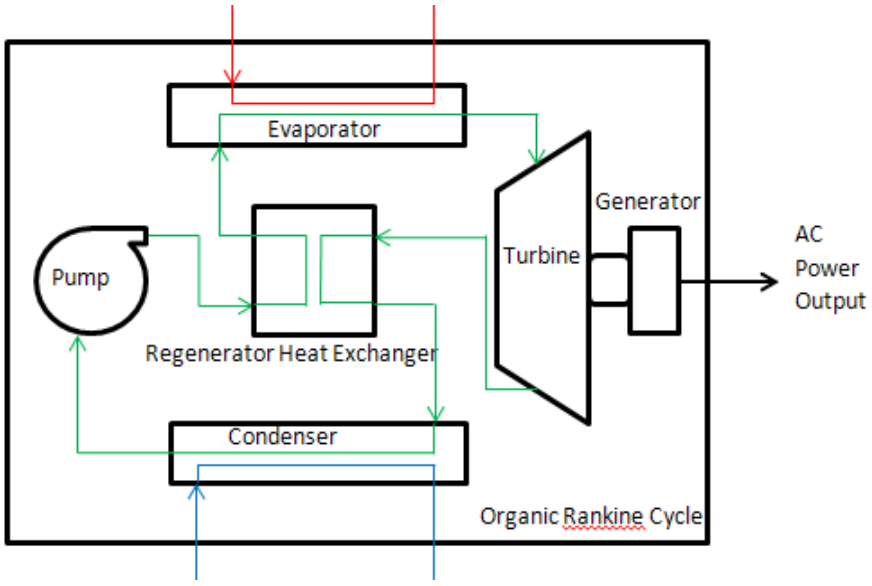

Figure 1.2: Organic Rankine Cycle with recuperator

The green line in Figure 1.2 corresponds to the organic fluid flowing within the organic Rankine cycle. The red line corresponds to the input waste heat, which can be in the form of a gas or a liquid. Usually thermal oil or water is used if the source is liquid. The blue line corresponds to the input cooling fluid, which is usually water from a reservoir or a nearby river.

There are four main components of an organic Rankine cycle (ORC). The first is the pump, which forces the organic fluid to flow through the cycle. The second is the evaporator which takes the waste heat as its input and transfers the heat to the working fluid which causes the fluid to change phase to a vapor. The third main component is the turbine generator combination which takes the working fluid vapor as the input and uses it to rotate a shaft which then produces power from the generator. The fourth component is the condenser which takes cold water as the input and transfers the heat from the working fluid to the cooling water. This causes the fluid to change phase back from a vapor to a liquid. The fifth component on this ORC is the recuperator heat exchanger which improves the efficiency of the cycle by taking more of the heat out of the working fluid before it is condensed and transferring the heat to the working fluid before it enters the evaporator. The problem with the recuperator is that it can only be used on certain types of working fluids. The different types of working fluids are defined by their slope on the vapor side of the saturation dome and will be discussed later. Only dry working fluids leave the evaporator before they have entered the two-phase state and their temperature is still much higher than the condensing temperature which means that they can transfer some of this heat to the working fluid

through the recuperator before they are condensed completely. This process is very similar to preheating in a boiler or furnace.

1.4 Literature Review

Many journal articles and research papers were read and studied in order to determine research that had already been performed in the field of organic Rankine Cycle technology. The literature read was mainly split into three categories: articles related to solar applications, articles related to the working fluids in ORC's, and articles related to the general working of ORC's. The first articles studied were those related to solar thermal applications of ORC's.

An article was written by M. Sloan, et al, which describes the testing and modeling of a SEGS LS-2 solar collector manufactured by Luz Technologies. The collector efficiency and thermal losses were compared with two types of receiver coatings and three different receiver configurations of a SEGS LS-2 parabolic trough plant. The configurations tested were: glass envelope with air, glass envelope with a vacuum, and a bare receiver. The coatings tested were a cermet coating and a black chrome coating. Equations were then derived to compare the thermal loses to wind speed, outlet temperature, and insolation values. The most efficient configuration was the glass envelope with a vacuum, followed by the glass envelope with air, and lastly the bare glass envelope. The most efficient coating was found to be the cermet.

The next article studied was written by H. Price and V. Hassani, and it describes an ORC system that was designed and optimized for a solar thermal application. An ORC power cycle was designed and optimized for use with a parabolic trough solar collector technology. A model was developed to enable the integration between solar and power cycles to determine the annual performance and power output of STORES. An economic assessment of plants and the cost of power were conducted.

An article was written by Reflective Energies, a DOE subcontractor, which developed an optimized ORC power cycle for integration with a parabolic trough solar field. Different working fluid options and different condensing options such as air-cooled and water-cooled were compared. A conceptual design and cost estimate for a 10 MWe Solar Thermal Organic Rankine Electricity System (STORES) was developed. A performance and economic assessment of initial and mature STORES plants was conducted. Preliminary market potential of STORES was investigated. The steps towards a demonstration or early commercial STORES project were laid out. Thermal storage options were also presented and discussed. Thermal storage options include but are not limited to: one-tank systems, one-tank thermocline systems, two tanks direct storage, and two tanks indirect storage.

An article written by SolarPaces describes an overview of parabolic trough power plants and discusses those already in operation. It briefly discusses the parabolic trough steam Rankine cycle as well as the integrated solar combined cycle system, which uses a coal powered steam cycle as back up when the sun isn't shining. It then provides a history on parabolic troughs and discusses the Luz LS-1, LS-2, and LS-3 power plants. It then lists multiple benefits and impacts of ORC's such as least cost for generated electricity, daytime peaking power, economically feasible, heat transfer fluid (HTF) spills, land, and water. Each existing large trough plant is compared in economics and performance.

The next type of articles investigated were those pertaining to the choice of working fluids within the ORC's. David Shroeder and Leslie Neil wrote an article that studied the effect of decomposition of working fluids in ORC's mainly based on temperature and use. Fluids were

chosen based on molecular weights, boiling temperatures, as well as temperature entropy curve designation. Results were based on theoretical calculations and previously recorded test results, no new testing was performed.

Written by Bo-Tau Liu and others their article studies the effects of various working fluids on the thermal efficiency and on the total heat recovery efficiency were studied in this report. It was found that hydrogen bonds in wet fluids were terrible candidates due to the larger vaporizing enthalpy and should not be used in ORC's. The thermal efficiency for various fluids was found to be a weak function of the critical temperature. It was also found that the maximum value of total heat recovery increases with an increase in inlet temperature of the waste heat source and it decreases with fluids having a lower critical temperature.

An article investigating the thermodynamic and physical properties of unconventional fluids for use in ORC's was written by V. Maizza and A. Maizza. These ORC's are evaluated under realistic design operation conditions. Some fluids studied are refrigerants, HCFC's, and mixtures of fluids. Choice of fluid depends on operating temperatures mainly. Graphs are given to select fluids based on temperature and design efficiencies.

In order to compare the operating characteristics of ORC's using different working fluids Tzu-Chen Hung performed multiple studies on how these fluids work in ORC's. Benzene, toluene, p-xylene, R-113, and R-123 were analyzed in an ORC and were compared by their efficiency, their irreversibilities, and the temperature of the heat source. P-xylene had the highest efficiency while Benzene had the lowest. P-xylene was shown the best at utilizing

waste heat from a high temperature heat source whereas R-112 and R-123 were best with low temperature heat sources. It was also shown that the irreversibilities mainly depend on the type of heat source, specifically vapor or liquid.

To obtain an understanding of how to analyze and interpret how an ORC is optimized and operated efficiently many articles were read on the general topic of ORC's. An ORC using R-245fa was analyzed and optimized using exhaust heat as the heat input source. This ORC is described in the journal article written by Dong Hong Wei, et al. The article found that increasing the mass flow of exhaust was the best way to effectively utilize all the waste heat available. It was also found that the fluid should be barely sub cooled when it exits the condenser. It was also found that ambient temperature played little role on the output of the system just mainly on the condenser, if it was air-cooled.

An experimental study is carried out on an ORC recovering heat from hot air at a temperature ranging from 150 to 200°C. This study was described in detail in Sylvian Quoilin's experimental modeling of small scale ORC's. The expander used for this study is a volumetric scroll expander. The working fluid selected is R-123 because of its high efficiency in ORC applications. During the testing period, the efficiency of the cycle and its output shaft power are increased. The limits of the cycle are investigated by modifying the hot air source temperature, expander rotational speed, and refrigerant charge. It turns out that the refrigerant charge has a tremendous importance in the behavior of the cycle and that its optimal value has to be found in order to maximize the performances.

Another study performed by Sylvain Quoilin was also used as a reference. This article contains a theoretical analysis of the thermodynamics within an ORC. First the variables are presented and defined then a first and second law analysis is performed on an ideal ORC. Optimizations and improvements in the cycle are discussed last.

1.5 Applications

Organic Rankine cycles (ORC's) can be used in a multitude of applications. Certain limitations exist on when and where an ORC can be used. ORC's can be implemented on almost any process that produces exhaust. The input for an ORC can be either a hot vapor or a hot liquid, although most manufacturers recommend that a hot liquid is used because it is easier to keep clean and has higher heat transfer ability. If the exhaust heat is in the gaseous state then it is best to run it through a gas to liquid heat exchanger and heat water or thermal oil to be pumped into the ORC. The minimum temperature that an ORC can run is about 160 degrees Fahrenheit and the maximum temperature is about 220 degrees Fahrenheit. Most manufacturers recommend the waste heat input to be about 200 degrees Fahrenheit. If the waste heat is above 220 degrees Fahrenheit it is not a problem because a heat exchanger can be implemented to lower the temperature down to the desired 200 degrees Fahrenheit. Many applications exist where the waste heat is greater than 200 degrees Fahrenheit most of them are in the manufacturing industry.

The biggest limitation to where an ORC can be installed is the mass flow rate of the waste heat. For example a 250 kilowatt ORC needs about 9 million BTU per hour input of heat at 200 degrees Fahrenheit. Examples of possible ORC implementations range from: rotary kilns used in concrete manufacturing, ovens used in pearlite manufacturing, prime movers- meaning big vehicles that are on for extended periods of time and have a high exhaust flow rate, as well as solar thermal applications.

The biggest savings can be seen in the manufacturing industry since the electricity produced can directly be used in the facility and the electricity does not need to be transmitted anywhere. When used in the manufacturing industry the electricity produced also greatly reduces the facility's demand since more electricity will be produced when the boilers or kilns are being fired at full load.

Solar thermal applications are also a big field for ORC's because the solar thermal system is already producing hot water which means there are no extra costs for heat exchangers and the water can be pumped directly into the ORC. Advantages to the solar thermal applications are that if a facility uses a lot of hot water a system can be oversized for the facility's need and the extra hot water can be used to run an ORC, which means the incentives are doubled since now the facility is implementing a solar thermal system and a micro turbine system.

The application of prime movers is the least likely area for implementation because most large vehicles such as barges or trains do not have a large enough flow rate to support and ORC. Prime movers are also an unlikely choice for ORC's because the exhaust is intermittent and dependent on the use of the vehicle. ORC's can also be implemented in biomass plants that are exhausting directly to the atmosphere. ORC plants like this currently exist in Germany. The most common implementation of an ORC is in the solar thermal field, due to the free heating of water from the sun. The main issue with this application is that the system needs to remain pressurized so the water does not turn to steam before it enters the ORC.

1.6 Fluid Selection

Efficient operation of an Organic Rankine Cycle is primarily a function of two parameters: the working conditions of the cycle and the thermodynamic properties of the working fluid used in the cycle. Three main types of working fluids exist that can be used in ORC's. These types are classified by their slope on the vapor side of the saturation curve. The plot in Figure 1.3 is a sample saturation dome that has been cut off after the inflection point in order to display the different type of fluid slopes. Figure 1.3 below shows a comparison of the types of fluids classified by their slopes on a T-s diagram. Note that this diagram does not directly reflect any specific fluids it is simply a graphic display of the possible types of fluids and their slopes.

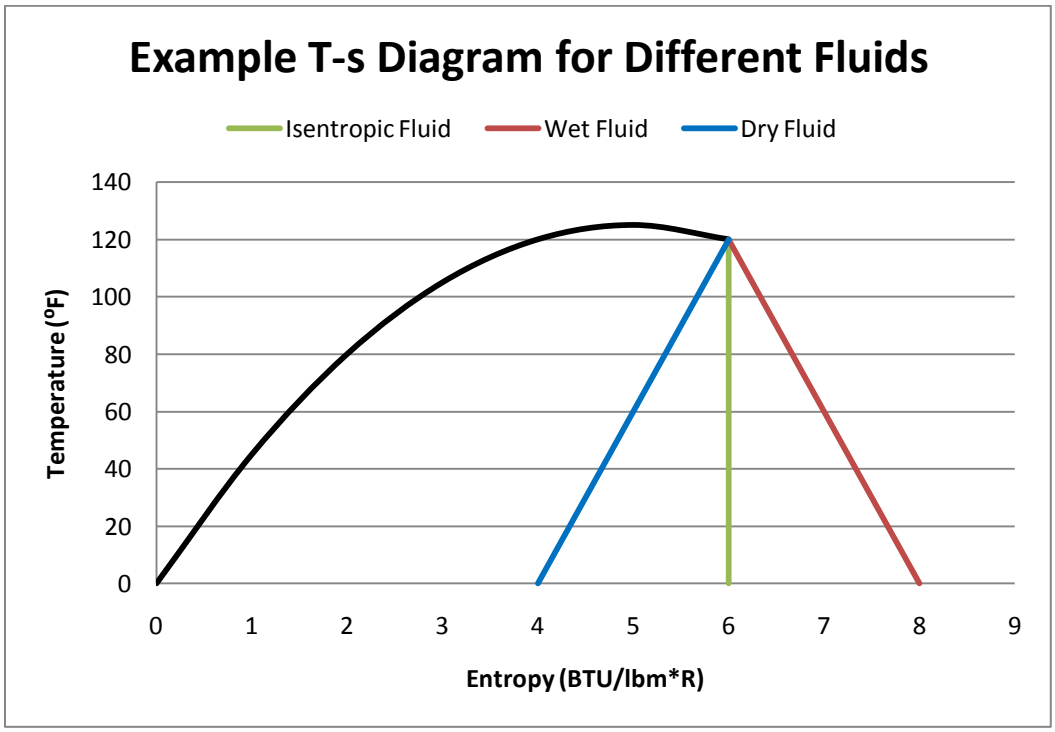

Figure 1.3: T-s Diagram for Different Fluid Types

A fluid that has a negative slope, such as the red line in Figure 1.3, is called a wet fluid. The most common wet fluid is water but other wet fluids include: ethanol, methane, hydrogen, and most fuels. A fluid that has a positive slope, such as the blue line in Figure 1.3, is called a dry fluid. Common dry fluids include: toluene, n-pentane, iso-pentane, R-245fa and many refrigerants. A fluid that has an infinite slope, such the green line in Figure 1.3, is called an isentropic fluid. Common isentropic fluids include: benzene, R-11, R-123, and hexane. The different types of fluids can alter the thermal efficiency of the ORC and each type can offer a different advantage when it is used within the cycle.

For instance, isentropic fluids are best at recovering low temperature waste heat whereas wet fluids are best at recovering high temperature waste heat and dry fluids are able to be used with a recuperator. The different types of fluids mainly affect the state of the working fluid at the exit of the turbine. Since the vapor-saturation curve for a wet fluid has a negative slope it is possible to be in a two-phase region after undergoing isentropic expansion in the turbine, if it is not highly superheated in the evaporator. This can be seen by drawing a vertical line starting at the pressure and temperature specified and ending at the final temperature and entropy. If this line lies in the saturation dome then it is possible that the fluid is still in the two-phase region. Since an isentropic fluid has an infinite slope on the vapor saturation curve the saturated vapor at the inlet to the turbine remains saturated throughout an isentropic expansion in an ideal turbine. Since a dry fluid has a positive slope on the saturation vapor curve when it undergoes an isentropic expansion in the turbine the fluid is superheated at the exit of the turbine.

A wet fluid, as seen in Figure 1.3, is the most unlikely choice for an ORC since it is most efficient utilizing high temperature waste heat. Wet fluids have a critical point which occurs at a far greater temperature then that of dry and isentropic fluids which makes them more efficient at higher pressures and higher temperatures. Since wet fluids have high molecular numbers they are more complex and have a higher ability to store heat than the less complex and lower molecular numbered dry fluids. A wet fluid is usually used to transfer heat from the waste heat source and from the cooling source to the ORC since it has a high heat capacity. This can be seen through the following equation.

The specific heat of a fluid can be rewritten as follows in order to relate temperature, entropy, and specific heat.

$$C_p = C_v + R = T * \left(\frac{\partial S}{\partial T}\right)_v + R \tag{1.1}$$

In the equation above; Cp is the specific heat of the fluid at constant pressure, Cv is the specific heat of the fluid at constant volume, T is the temperature of the fluid at a given state, and $\left(\frac{\partial S}{\partial T}\right)_v$ is the partial derivative of entropy with respect to temperature at a constant volume. By comparing the slopes on the vapor side of the saturation dome for wet and dry fluids one can see that the slope for a dry fluid is a much steeper than the slope for a wet fluid. In a T-s diagram the slope is the change in temperature divided by the change in entropy. This relation is the inverse of the term in equation 1.1. Since the inverse of a large number is very small, a fluid with a steep slope would have a lower Cp than a fluid with a gradual slope. This shows that wet fluids have a higher heat capacity than dry fluids and

should be used in higher temperature situations or applications that require a lot of heat to be delivered to a source.

The main advantage of using a dry fluid is that a recuperator heat exchanger can be used in the cycle to take the energy left in the superheated vapor at the exit of the turbine and use it to preheat the fluid entering the evaporator. The use of a recuperator increases the overall thermal efficiency of the cycle and reduces the amount of heat input and output to and from the cycle. Turbines are easily damaged by moisture contained in the vapor that is expanded in the turbine. Dry fluids cause less damage on turbines, compared to wet fluids, since they are superheated throughout the expansion within the turbine. This is a great advantage to dry fluids since the wear and tear on the turbine is less which yields and overall longer life of the turbine.

An isentropic fluid is very efficient at recovering low temperature waste heat and may be the best choice of working fluid depending on whether a recuperator is desired. Isentropic fluids have a lower critical temperature than wet fluids which makes them more efficient at recovering low temperature waste heat than wet fluids. The overall area within the saturation dome is greater for an isentropic fluid than a dry fluid. This means that the maximum work achievable by a cycle using an isentropic fluid is greater than that of a dry fluid. The choice of the working fluid greatly affects the thermal efficiency of the ORC. According to a study done by T.C. Hung et al, the efficiency of the cycle is closely related to the latent heat of the fluid at low pressure; a greater latent heat at low pressure yields a lower efficiency since a larger portion of the energy carried by the fluid is rejected via the condenser. The efficiency

is also a weak function of the turbine inlet temperature, i.e. an increase of superheat in the turbine does not result in a significant increase in efficiency.

The efficiency of the ORC increases nearly linearly with the turbine-inlet temperature. Unlike wet fluids, dry fluids show decreased efficiency as the turbine-inlet temperature is increased, except when the system pressure is very high. This result indicates that the optimum efficiency occurs if dry fluids operated along the saturation curve without being superheated.

Isentropic fluids exhibit trends similar to wet fluids except that the increase of efficiency levels off as the temperature is increased. The system efficiency also increases as the system pressure increases. The working fluid yields more work during the isentropic expansion process if the turbine-inlet pressure is raised. However, raising the system pressure is not always feasible for economic reasons since the capital costs for the waste-heat boiler and piping system, as well as system complexity and material selection of the components, must also be considered. [Hung et al]. Therefore the choice of the working fluid depends greatly on the desired outcome of the ORC, i.e. if a recuperator is desired, if higher output is desired, or if higher thermal efficiency is desired.

1.7 Manufacturers:

Ormat is a world leader of geothermal power plant technology and has developed the Ormat Energy Converter (OEC). The OEC is essentially a commercially available ORC that is used in waste heat applications. OEC's can be purchased in sizes ranging from 250 kW to 20 MW. The OEC can be either air-cooled or water-cooled but must have a liquid as the heat input to the OEC. The OEC turbines are moisture free and operate at about 1500 rpm with a very high efficiency. The OEC uses a dry refrigerant as the working fluid and does not incorporate a recuperator. Ormat would not divulge the operating characteristics or exactly which dry refrigerant they were using.

Infinity Turbine is a small, relatively unknown company that manufactures turbines and ORC systems. Infinity Turbine sells ORC's in the range of 1 kW up to 250 kW. The smaller systems are build/design your own system where you can purchase the components separately and build it yourself and the larger systems are almost turnkey systems where the ORC can be installed and operated. Infinity Turbine uses R-245fa as the working fluid and the operating conditions vary depending on the size of the system purchased. The ORC's sell for about $1500/kW and require liquid as the heat input and as the cooling medium. Most of the ORC's incorporate a recuperator.

Turboden is a division of Pratt and Whitney that is devoted to clean energy production and is based out of Italy. Turboden has ORC heat recovery units available from 400 kW to 5 MW. Turboden's ORC's prefer thermal oil as the heat input, but can use water, and require a water-cooled condenser. All of Turboden's units are equipped with recuperators and claim to

be about 20% efficient. Turboden uses a variety of working fluids in their ORC's and can be modified for the customers exact specifications.

Electratherm is a company devoted to energy conservation and sustainability. They have designed a product called the Green Machine that is essentially a turnkey ORC system. The Green Machine requires the heat input to be in liquid form, preferably water, and a water-cooled condenser. The Green Machine's advantage versus other competitors is that it incorporates a double screw expander that is supposedly more efficient than standard expansion turbines. The Green Machine has multiple working fluids available to be used depending on the application and claims to have a 3-year payback. The units vary from about 30 kW to 200 kW.

CHAPTER 2

2.1 Theoretical Comparison:

The operating conditions of an ORC can greatly affect how efficient the cycle is. The main factors affecting the efficient operation of an ORC are the maximum temperature, the maximum pressure, the amount of heat input, and work output from the system. In order to compare how efficient a cycle operates at these different conditions the thermal efficiency can be calculated for each condition and compared. Since many operating points for these cycles exist a theoretical ORC was designed and analyzed multiple times. The cycle was analyzed for three different fluids. For each fluid, the cycle was analyzed at multiple boiler pressures within the system. For each pressure of each fluid multiple iterations were performed to analyze the cycle under different operating conditions. Several different iterations were performed for each pressure of each fluid and only one aspect of the cycle was changed each time it was analyzed.

The tables below show the number of iterations and the parameters altered for each fluid and each pressure. Table 2.1, 2.2, and 2.3 are for R-245fa, R-245ca, and R-123 respectively. Tmax and P max refer to the temperature and the pressure in the boiler of the ORC.W out refers to the work output of the turbine, and m dot is the mass flow rate of the refrigerant within the cycle. The control run, iteration number 1, has the work output set to 250 kW and a mass flow rate of 27.8 lbm/min. These are considered to be the default values and are held constant except when the temperature and pressure are varied.

Table 2.1: Iterations and Altered Parameters for Theoretical Analysis (R-245fa)

	Fluid	R-245fa			
Iteration #	**P max**	150 Psia	125 Psia	100 Psia	75 Psia
1	**Tmax**	Tsat	Tsat	Tsat	Tsat
2	**Tmax**	Tsat + 5^0F	Tsat + 5^0F	Tsat + 5^0F	Tsat + 5^0F
3	**Tmax**	Tsat + 10^0F	Tsat + 10^0F	Tsat + 10^0F	Tsat + 10^0F

Table 2.2: Iterations and Altered Parameters for Theoretical Analysis (R-245ca)

	Fluid	R-245ca					
Iteration #	**P max**	100 Psia	90 Psia	80 Psia	70 Psia	60 Psia	50 Psia
1	**Tmax**	Tsat	Tsat	Tsat	Tsat	Tsat	Tsat
2	**Tmax**	Tsat + 5^0F	Tsat + 5^0F	Tsat + 5^0F	Tsat + 5^0F	Tsat + 5^0F	Tsat + 5^0F
3	**Tmax**	Tsat + 10^0F	Tsat + 10^0F	Tsat + 10^0F	Tsat + 10^0F	Tsat + 10^0F	Tsat + 10^0F

Table 2.3: Iterations and Altered Parameters for Theoretical Analysis (R-123)

	Fluid	R-123					
Iteration #	**P max**	87 Psia	80 Psia	70 Psia	60 Psia	50 Psia	45 Psia
1	**Tmax**	Tsat	Tsat	Tsat	Tsat	Tsat	Tsat
2	**Tmax**	Tsat + 5^0F	Tsat + 5^0F	Tsat + 5^0F	Tsat + 5^0F	Tsat + 5^0F	Tsat + 5^0F
3	**Tmax**	Tsat + 10^0F	Tsat + 10^0F	Tsat + 10^0F	Tsat + 10^0F	Tsat + 10^0F	Tsat + 10^0F

Many assumptions were made to accurately compare the operating points of the cycles. The main comparison point was the thermal efficiency of the cycle since that is a large limiting factor of how much waste heat can be converted into electricity. The program RefProp was used to evaluate the thermodynamic properties of the working fluids at different points within the cycle. RefProp is a program built by NIST that can evaluate the properties of many different fluids. RefProp can also be used to plot a number of different thermodynamic properties for fluids such as a temperature versus entropy graph. The assumptions made are summarized in Table 2.4 below.

Table 2.4: Theoretical Analysis Assumptions

Ideal	s4=s3 P2=P3 P4=P1	
M dot	0.100	(10^6)lbm/hr
	27.778	lbm/s
W dot gen	0.853	MMBTU/hr
	250	kW
Q dot in	9	MMBTU/hr

The first assumption was that the cycle was ideal. This was assumed so that irreversibilites within the cycle were negligible and only ideal theoretical conditions were considered. The ideal assumption implies the following four steps to the cycle: isentropic compression in the pump, constant pressure heat addition in the boiler, isentropic expansion in the turbine, and constant pressure heat rejection in the condenser. The states used to evaluate the cycle are defined as: state one is the point at the outlet of condenser and the inlet of the pump, state two is the point at the outlet of the pump and the inlet to the boiler, state three is the point at

the outlet of the boiler and the inlet to the turbine, state four is the point at the outlet of the turbine and the inlet to the condenser. These states and a sample T-s diagram can be seen below in Figure 2.1.

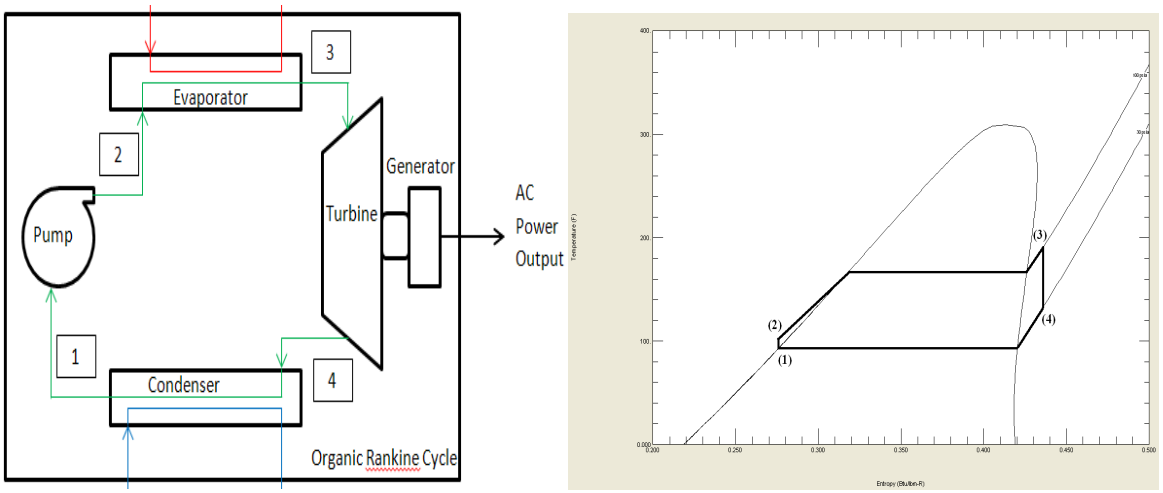

Figure 2.1: T-s diagram and State Points

The Carnot efficiency of a theoretical heat engine operating between a 200^0F high temperature heat reservoir and a 55^0F low temperature reservoir was calculated. This was done through equation 2.1 below and was used to compare the calculated thermal efficiency.

$$\eta_{carnot} = 1 - \frac{T_c}{T_h} = 1 - \frac{515\ R}{660\ R} = 0.22 \tag{2.1}$$

The Carnot efficiency was found to be approximately 22%. The calculated thermal efficiency of the cycle does not exceed 10% which means that the cycle does not violate any physical laws.

The theoretical analysis was performed for a 250 kW system. This was chosen because manufacturer's data was available for this unit and this unit was used in a recent IAC recommendation, therefore the cycles could be compared. This assumption means that the work output from the turbine would be 250 kW. Note that the efficiencies of the turbine and the generator were neglected since this is an ideal theoretical analysis. The heat transfer rate from the waste heat to the input of the boiler was assumed to be constant and a value of 9 MMBTU/hr. This value was chosen based on a manufacturer's recommendations that stated that the power output would be equal to the heat transfer rate, in BTU/hr, divided by about 35000 BTU/hr*kW depending on the temperature of the heat source and the mass flow rate of the fluid. From equation 2.2 it can be seen that for a 250 kW output about 9 MMBTU/hr is required.

$$Qinput = 250kW * 35{,}000\frac{BTU}{kWh} = 9 * \frac{10^6 BTU}{hr} \tag{2.2}$$

The mass flow rate of the working fluid was also assumed to be about 28 lbm/s. This was chosen based on a manufacturer's recommendations. It was also assumed that the heat input would be at 200 degrees Fahrenheit, since that is the maximum temperature at which an ORC using R245fa can efficiently operate.

In order to calculate the specified state points within the cycle the first law of thermodynamics was applied to the system. The first law of thermodynamics in equation form is shown below in equation 2.3.

$$\Delta E = (Q_{in} - Q_{out)} - (W_{out} - W_{in}) = 0 \tag{2.3}$$

Where delta E is the change in energy which is equal to zero for a cycle, Q_{in} is the heat added to the boiler from the waste heat application, Q_{out} is the heat rejected to the environment from the condenser, W_{out} is the work produced by the turbine generator combination, and W_{in} is the work required by the pump to move the working fluid.

The analysis began with state three, the outlet to the boiler. Since it was desired that the fluid be in vapor form at the exit of the turbine the quality of state three was specified to be one. The pressure for the first iteration of the analysis was chosen as the saturation pressure of the fluid when the temperature was close to the theoretical input temperature of 200 degrees Fahrenheit. The temperature of state three was then assumed to be the temperature at which the quality was one and the pressure was equal to the saturation pressure. With two independent properties defined, RefProp could be used to determine the enthalpy, density, specific heat, and entropy of the fluid at state three. Since state three was determined and the work output desired from the turbine as well as the mass flow rate of the refrigerant was known, state four's properties could be calculated. Using the ideal assumption that the expansion in the turbine happens isentropically the entropy in state four should be equal to the entropy in state three. Another independent property is still required to calculate all the variables within state four. To calculate this needed variable the work of the turbine was used and the equation for work output from a cycle was modified and is shown in equation 2.4 and 2.5 below.

$$W_{out} = m_{dot} * (h_4 - h_3) \tag{2.4}$$

$$h_4 = h_3 - \frac{W_{out}}{m_{dot}} \tag{2.5}$$

Now that the enthalpy and entropy of state four was known all the other properties could be obtained through RefProp.

Next state two's properties were determined through a similar analysis as state four. Since the heat input added to the boiler was known and the ideal assumption implies that the pressure at state two would be equal to the pressure at state three all the properties at state two were able to be calculated. In order to calculate the enthalpy at state two the following equations were used.

$$Q_{in} = m_{dot} * (h_3 - h_2) \tag{2.6}$$

$$h_2 = h_3 - \frac{Q_{in}}{m_{dot}} \tag{2.7}$$

Now that state two's enthalpy and pressure were known the remaining properties could be obtained using RefProp. State one's properties are the only ones left to be determined now. State one's properties could be calculated in two different ways. The first way to do this was using the ideal assumption again. The heat rejection happens at a constant pressure therefore the pressure at state one is equivalent to the pressure at state four. The pumping happens at constant entropy which means that state one's properties can be defined by the two independent properties of entropy and pressure. The problem that arises by using this assumption is that sometimes the quality at state one based solely on the entropy and pressure was not always zero. This is a problem because the fluid should be in liquid form when it exits the condenser at state one. The second way to determine state one is similar to the process used to define state three. The pressure in state one is assumed to be equivalent to the

pressure in state four, just like the previous step, but instead of using the entropy value that is equivalent to state two's entropy the quality is assumed to be zero which causes the temperature to be the saturation temperature at that given pressure. This has a very small effect on the ideal cycle assumption because the values of entropy calculated both ways were within 5% difference of each other.

Now that the cycle had been evaluated at each specified state point, the first law of thermodynamics was checked to make sure that no energy was created or destroyed. The thermal efficiency was then calculated through the following equation.

$$\eta_{thermal} = 100 * \left(1 - \frac{(h_1 - h_{4)}}{(h_2 - h_3)}\right) = \frac{W}{Qin} = \frac{Qout - Qin}{Qin} \quad (2.8)$$

This theoretical analysis was performed for multiple operating conditions and multiple working fluids. The three fluids investigated and compared were R-245fa, R-245ca, and R-123. These fluids were chosen because they are all dry fluids and they all are used in commercially available ORC's. The dry fluids were chosen because these types of fluids have the highest efficiencies in ORC's due to the fact that the fluids are inherently superheated at the outlet of the boiler based on the temperature versus enthalpy diagrams of the fluids.

Once the fluids were selected each fluid was analyzed at a range of boiler pressures, temperatures, flow rates, and assumed power. These specified operating conditions are shown in Tables 2.1, 2.2, and 2.3. All the pressures listed correspond to the maximum pressure in the system which is also the pressure at state three or the boiler pressure. The

analysis was then carried out for each fluid where the boiler pressure and temperature was varied multiple times. The temperatures investigated were the saturation temperature at the given pressure, the saturation temperature plus five degrees, and the saturation temperature plus ten degrees. For the next iterations the temperature was set to the saturation temperature and the assumed power was varied from 150, to 250, to 300, to 500 kW. The last iterations were looking at the effect of mass flow rate on the thermal efficiency. This was done by setting the boiler temperature to the saturation temperature and decreasing the value of the mass flow rate. It was attempted to increase the flow rate as well but many problems occurred when this happened.

Figure 2.2 below shows the effect of the variation of maximum temperature on the thermal efficiency of a theoretical ORC using R-245fa as the working fluid.

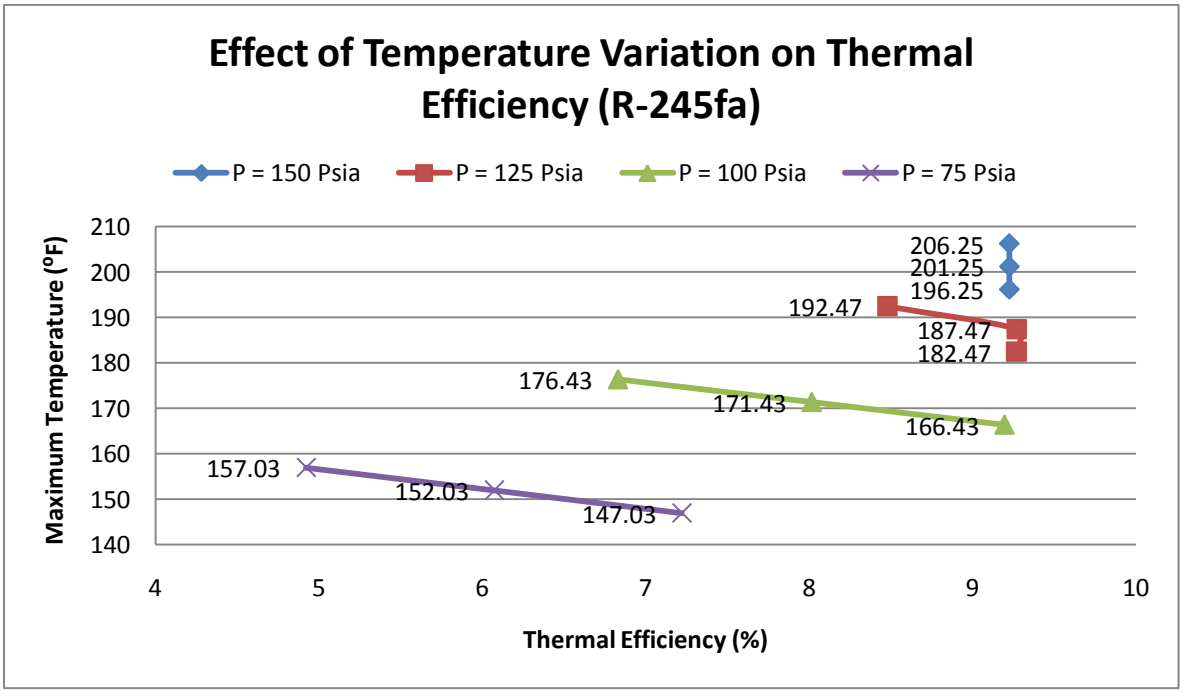

Figure 2.2: Temperature Variation on Thermal Efficiency (R-245fa)

The above plot shows the thermal efficiency for a 250 kW ORC using R-245fa as the working fluid. The thermal efficiency was calculated at three different temperatures for four different operating pressures. Overall it can be seen that the higher the boiler pressure leads to an overall higher thermal efficiency. Since the pressure is proportional to the temperature in the cycle it is expected that the lower pressure will have a lower temperature which would mean that the fluid doesn't absorb as much heat as it would at a higher pressure and would ultimately have a lower thermal efficiency. This claim is supported by Figure 2.2 shown above. It was also expected that increasing the temperature within the boiler while keeping the pressure within the boiler constant would cause the thermal efficiency to decrease. This is also seen in the plot above. This is mainly due to the heat input being increased while the work output remains constant which leads to a decrease in thermal efficiency. It was expected that each pressure grouping would follow the same trends for the increases in maximum temperature but this is not the case. For a pressure of 150 psia there is almost no change in thermal efficiency with an increase in maximum temperature, and is constant at 9.22%.

For a pressure of 125 psia there is a unique nonlinear decrease in thermal efficiency with an increase in maximum temperature. With an increase of five degrees Fahrenheit each time the thermal efficiency first increases by 0.0001% then decreases by about 0.8%. This shows that there is an optimum temperature and pressure that can be found for each operating condition for each ORC.

The next two pressures, 100 and 75 psia displayed expected trends of a linear decrease in thermal efficiency with a linear increase in maximum temperature. It was calculated that for each degree Fahrenheit increase above the saturation temperature the thermal efficiency decreases by about 0.23%.

This process was repeated for other working fluids; the results are shown and discussed below. In Figure 2.5, the effect of thermal efficiency on an ORC using R-245ca as the working fluid is shown as the maximum temperature is varied.

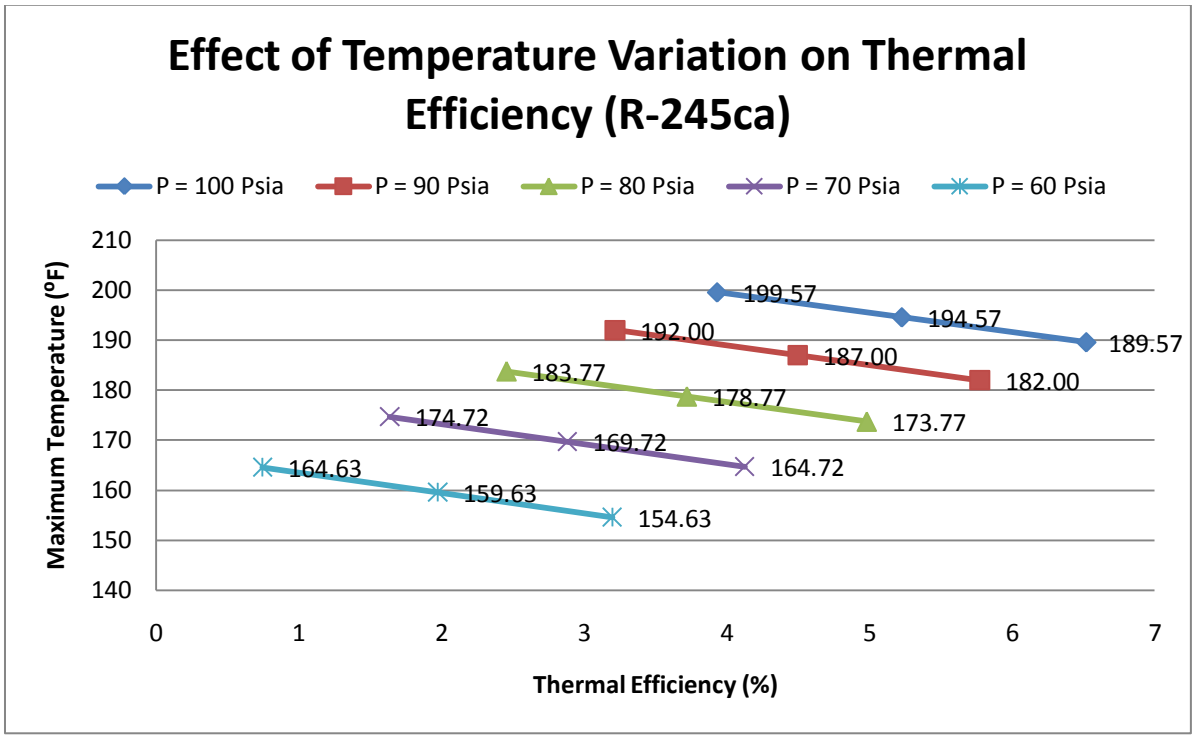

Figure 2.3: Effect of Temperature Variation on Thermal Efficiency (R-245ca)

The fluid of R-245ca was chosen to directly compare it to the more commercially used R-245fa. R-245ca has a smaller range of pressures available than R-245fa which means that it

was evaluated at every 10 Psia instead of every 25 psia. R-245ca cannot be used above 100 psia since the temperature of the fluid would exceed the maximum temperature allowed in the cycle. This shows that the fluid would be more efficient in higher temperature waste heat applications, such as a solar thermal ORC. The trends shown in the above plot are consistent with those expected, and show a decrease in thermal efficiency with an increase in maximum temperature for each given pressure. The trend shown in Figure 2.5 above is the same as the trend shown with R-245fa at low working pressures but the trend shown in the higher pressures of the R-245fa analysis are not seen. This could be due to the fact that the cycle has been evaluated at below optimum conditions and the best operating point for this working fluid has not been found. It could also be that the trends shown in the first analysis of R-245fa were flawed in some way. The maximum efficiency shown in Figure 2.5 is about 7% which is far below the maximum efficiency seen when using R-245fa as a working fluid. Since the ORC in the previous study, using R-245fa as the working fluid had a maximum efficiency of about 10% it is assumed again that R-245ca could be utilized in a more efficient method if higher temperature heat sources were used.

The same analysis was again performed for another dry refrigerant, R-123. The results for each iteration and analysis of an ORC are shown below using R-123 as the working fluid within the cycle. In Figure 2.8 it is shown that the thermal efficiency of the cycle is affected by varying the maximum temperature within the ORC.

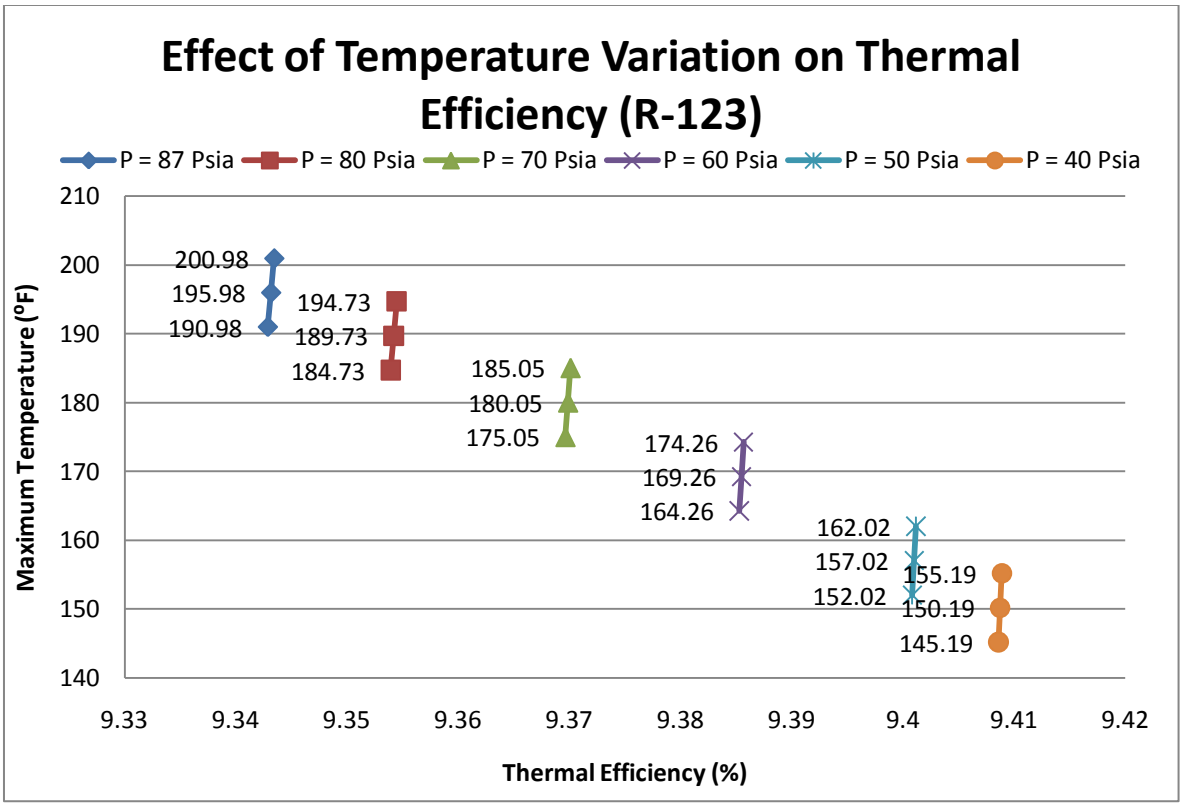

Figure 2.4: Effect of Temperature Variation on Thermal Efficiency (R-123)

The plot of thermal efficiency versus maximum temperature variations for R-123 is very different than the graphs for previous working fluids. The plot for R-123 shows a constant trend for each chosen pressure similar to the R-245ca graph, but the R-123 plot shows the opposite trend that R-245ca. The trend shown in Figure 2.8 shows that as the maximum temperature in the cycle is increased the thermal efficiency increases as well. Even though the graph appears to show the efficiency increasing the values of thermal efficiency only increase by about 0.01% with an increase of 10 degrees Fahrenheit in the maximum temperature. Since the thermal efficiency remains relatively constant for each temperature setting this means that for the working fluid of R-123 the thermal efficiency of the cycle is a

weak function of the maximum temperature in the cycle. This plot is also different than the previous fluids because with the previous fluids the higher pressures had overall higher thermal efficiencies than the lower pressures, this is not the case for R-123. R-123 shows that the lower pressures have a higher thermal efficiency. This leads to the assumption that R-123 is better suited for ORC's that operate at lower pressure. ORC's that operate at a lower pressure inherently operate at a lower temperature because the saturation temperature of the fluid is decreased when the pressure is decreased. Even though the thermal efficiency of R-123 shows different trends than the previous working fluids its efficiency is still not as high as the efficiency of the ORC using R-245fa as the working fluid.

Overall it can be seen that the operating conditions of the ORC's are mainly defined by the temperature and the pressure within the boiler. The thermal efficiency for the cycle appears to be very dependent on the working fluid rather than the operating conditions of the ORC. It was also found the R-245fa is the most consistently efficient working fluid for small-scale operation. Using R-123 as the working fluid is most efficient when the pressure or temperature is lowest and using R-245ca is most efficient when the pressure or temperatures are very high. The maximum thermal efficiency was found using R-123 at a pressure of 87 psia and a work output of 500 kW. The lowest efficiency was found to be using R-245ca at a pressure of 50 psia and a work output of 500kW.

Now that the entire cycle was analyzed theoretically and no efficiencies or loses were taken into account, all the iterations of the cycle was analyzed using isentropic efficiencies for the pump and the turbine. This was done to get a more realistic idea of the efficiency and

operating points of the ORC system. The pump was assumed to have an isentropic efficiency of 80% and the turbine was assumed to have an isentropic efficiency of 70%. The definition of isentropic efficiency for a pump and a turbine were modified to calculate the actual values of the working fluid at state points two and four. Equation 2.9 below shows the definition of isentropic efficiency for a turbine.

$$\eta_{isent\_T} = \frac{h_3 - h_{4a}}{h_3 - h_4} \tag{2.9}$$

$$h_{4a} = h_3 - \eta_{isen\_T} * (h_3 - h_4) \tag{2.10}$$

Equation 2.10 shows equation 2.9 solved for the actual enthalpy of the fluid at state 4. The subscripts in the equation correspond to the state points of the cycle where 3 and 4 are the ideal values and 4a is the actual value. These equations can be applied to the pump if the states are moved from 3 and 4 to states 1 and 2 respectively. These equations are shown below.

$$\eta_{isent\_P} = \frac{h_1 - h_{2a}}{h_1 - h_2} \tag{2.11}$$

$$h_{2a} = h_1 - \eta_{isen\_P} * (h_1 - h_2) \tag{2.12}$$

The main difference between the equations for the pump and the turbine are the state points used and the value of the isentropic efficiency. The analysis of the cycles and the parameters altered remained constant. The equations for enthalpy were the only thing that changed. After

the cycles were analyzed isentropically the thermal efficiencies and energy balances were compared to the completely theoretical results found earlier.

It was found that the addition of the isentropic efficiencies of the pump and the turbine did not affect the trends exhibited in the ideal graphs. The only thing affected were the values of the thermal efficiency, work output, work input, heat input, and heat output. On average the thermal efficiency was decreased by about 30.7%. This is the same amount that the efficiency of the turbine was decreased by which means that thermal efficiency and isentropic efficiency of the turbine have a linear relationship. On average it was found that the work output and input were increased by exactly 30%. This means that the work output is proportional with the isentropic efficiency of the turbine. This also holds true for the work input since it is proportional to the work output. The heat input was found to increase by an average value of 1.15% whereas the heat output was found to increase by an average value of about 3.37%. It was also found that the isentropic efficiency had more of an effect on the cycle at higher pressures. The isentropic efficiency was also found to have the same effect on the energy balance of the cycle at different boiler temperatures. This means that the isentropic efficiency of the turbine and pump are a stronger function of pressure than temperature. This can be verified since the enthalpy of a fluid is a stronger function of pressure than temperature. It was also found that varying the fluid had little effect on the changes in thermal efficiency. This is thought to be true since the decrease in work output is based on the percentage decrease in isentropic efficiency and not on each fluid specifically.

Overall using isentropic efficiencies an ORC is only about 6 to 8% efficient. This seems terribly low for a power producing apparatus, but since the cycle is designed to convert waste heat into electricity all of the power is essentially free power that would otherwise be wasted into the atmosphere.

An analysis was also performed on a theoretical cycle again to plot the T-s diagrams of the system for three different fluids. To calculate the state points for the cycle three assumptions were made; the boiler pressure was assumed, the boiler temperature was set to 200˚F because that would be the maximum theoretical temperature available, and the condenser pressure was assumed. Since the boiler pressure and temperature were assumed the remaining properties for state three could be calculated. Next the properties at state one were calculated by setting the pressure in the condenser and specifying that the fluid would be completely condensed liquid. Now that two the pressure and quality were known the remaining properties for state one could be calculated. The work input of the cycle was calculated through the following equation.

$$w_{in} = \frac{1}{\rho} * (P_3 - P_1) \tag{2.13}$$

In equation 2.13; w_{in} is the work input required by the pump, ρ is the density of the fluid, P_3 is the boiler pressure, and P_1 is the condenser pressure. This analysis was performed on a mass basis and the units are in BTU/lb.

The remaining properties were determined by using the ideal cycle assumption of constant pressure heat addition/rejection and isentropic compression/expansion. Therefore the

pressure and entropy at state two and four were known. Once all the state points were found an energy balance was performed on the cycle to calculate the work input, work output, heat input, heat output, thermal efficiency, and Carnot efficiency. The heat input/output was calculated through the enthalpy difference between the two state points as well as the work input. To determine the actual properties ate state two and state four, an isentropic efficiency of the turbine was set to 85% and the isentropic efficiency of the pump was set to 87%.

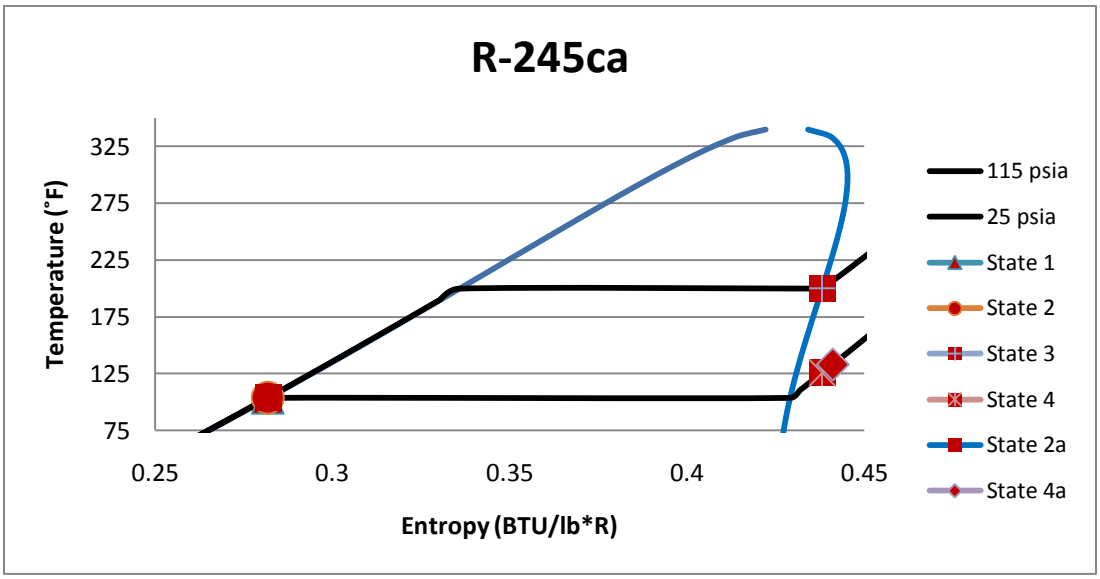

Figure 2.5: R-245ca T-s Diagram

The plot above shows the T-s diagram for R-245ca. It can be seen that the cycle was operating between 115psia and 25psia. The work output was found to be 10.996 BTU/lb, with a heat input of 100.477 BTU/lb. This leads to a thermal efficiency of about 10.5%. Since the cycle was operating between 200˚F and 103˚F the Carnot efficiency was about 14.6%. Therefore the cycle is operating at about 71.7% of the Carnot efficiency.

The next fluid analyzed was R-245fa. It was found that the cycle was most efficient operating between 157psia and 58psia. This leads to a temperature range between 200˚F and 130˚F. The cycle with R-245fa has a Carnot efficiency of about 10.5% and a thermal efficiency of 7.6% this means that the cycle is operating at about 72.8% of the maximum possible efficiency. The work output was found to be about 7BTU/lb with a heat input of 85.2BTU/lb. The temperature entropy diagram for R-245fa is shown below.

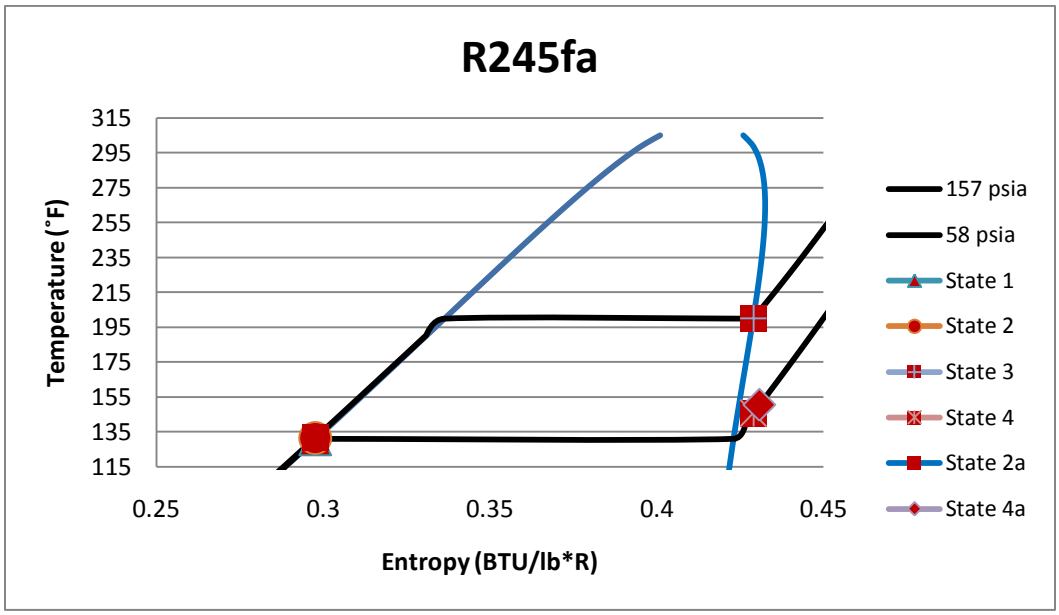

Figure 2.6: R-245fa T-s Diagram

The last fluid analyzed was R-123. It was found that the cycle was most efficient operating between 97psia and 42psia. This leads to a temperature range between 200˚F and 140˚F. The cycle with R-123 has a Carnot efficiency of about 9% and a thermal efficiency of 6.8% this means that the cycle is operating at about 75.5% of the maximum possible efficiency. The

work output was found to be about 5.3BTU/lb with a heat input of 74.8BTU/lb. The temperature entropy diagram for R-123 is shown in figure 2.13 below.

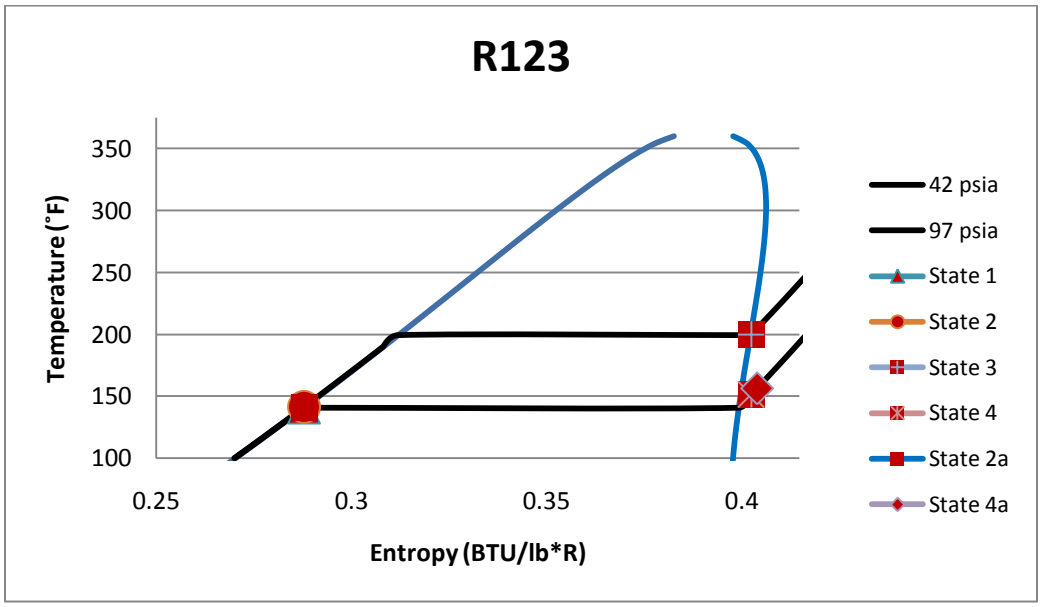

Figure 2.7: R-123 T-s Diagram

Overall it can be seen that the cycle using R-245ca as the working fluid has the highest thermal efficiency of the three fluids, at 10.5%. Although R-245ca has the highest thermal efficiency as well as highest work output and heat input, it has the highest percent difference between the actual thermal efficiency and the Carnot efficiency. Using R-245fa as the working fluid produces more moderate results. R-245fa can produce more power than R-123 but has a similar percent difference between the actual thermal efficiency and the Carnot efficiency. R-123 is the lowest of the three fluids. It has the lowest thermal efficiency, work output, and heat input. R-123 shows the lowest percent difference between the thermal

efficiency and the Carnot efficiency. An appropriate fluid should be chosen based on the pressure and heat requirements for the desired application.

2.2 Cycle-Tempo

Cycle-Tempo is a program developed and designed by the TU Delft (Delft University of Technology) to analyze and optimize thermodynamic systems used for the production of heat, electricity, and refrigeration. Cycle-Tempo is a graphical user interface type of program in which the user drags components of the cycle to the center of the screen and then connects them with pipes containing user specified types of fluids. Cycle-Tempo can be used for many different applications such as: steam turbine cycles, STAG units, gas turbine cycles combustion and heat transfer systems, coal and bio mass gasification combined cycles, fuel cell systems, and organic Rankine cycles. Cycle-Tempo was used to model and optimize the most efficient ideal cycle found in the theoretical analysis.

Cycle-Tempo requires the user to input the specified pressures and temperatures for certain apparatuses within the cycle then it calculates the optimum mass flow rate for the cycle. It also calculates the efficiencies of each apparatus as well as thermodynamic loses in each pipe and performs an energy balance on the each apparatus within the cycle. Cycle-Tempo can also be used to generate T-S diagrams, Mollier plots, Q-T diagrams, and value diagrams for various components of the system or for the entire cycle. Cycle-Tempo requires the international system of units to be used.

The ORC modeled in Cycle-Tempo was based off of the theoretical calculation of an ORC using R-245fa as the refrigerant that was designed to produce about 300 kW of electricity. This ORC was modeled in Cycle-Tempo then a recuperator was added in an attempt to

increase the thermal efficiency of the cycle. Figure 2.11 below shows the model of the ORC without the recuperator.

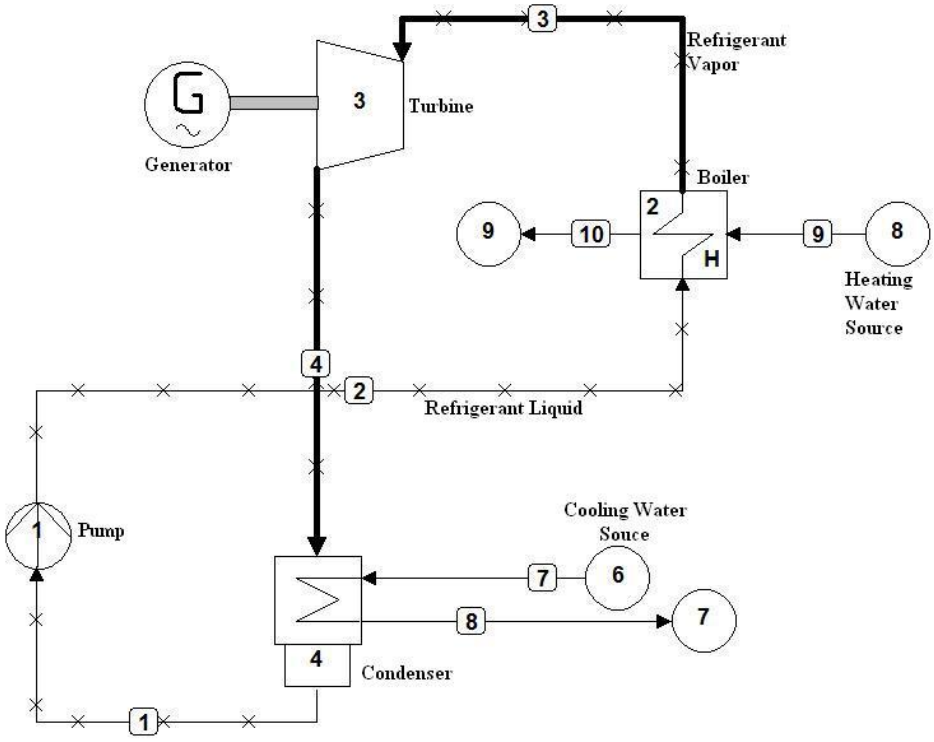

Figure 2.8: Cycle-Tempo ORC model

In the model above the numbers on the pipes correspond to the same state points as in the theoretical analysis; state one is at the inlet to the pump, state two is at the inlet to the boiler, state three is at the inlet to the turbine, and state four is at the inlet to the condenser. The pipes with the "X's" on them correspond to pipes containing R-245fa; the bold pipes with "X's" contain R-245fa in vapor phase whereas the normal lines with "X's" contain liquid R-245fa. The pipes that have no "X's" on them contain water used for the heat input to the boiler and the cooling input to the condenser. The symbol with a number three on it is the

turbine and is connected by a shaft to the generator, which is the symbol with the "G" on it. Apparatus number two is the boiler, which is modeled as a heat exchanger with a constant heat input from hot water. Apparatus number one is the pump and apparatus number four is the condenser that is modeled with a constant cooling input from a water tank. The symbols that are circles, numbers 6, 7, 8, and 9, are heat sources and sinks. Heat source eight is modeled as the waste heat source which has a constant specified temperature and a specified mass flow rate. Heat sink six is modeled as the cooling water source, in this case a water tank at a constant specified temperature and a constant specified mass flow rate. Heat sinks nine and seven are used as outlets for the cooling/heating water. In reality the heating and cooling water for the ORC are contained in their own loops and do not have two heat sinks. The water is usually contained in a tank and just re-circulated throughout the loop but since the analysis and modeling was to investigate the ORC and not the sources of cooling or heating they were modeled as simple heat sources and sinks.

In order to accurately model the 300 kW cycle analyzed earlier the temperatures and pressures used in the theoretical analysis were input to Cycle-Tempo in the following order. First the model was constructed and the apparatuses were connected with pipes containing the desired working fluid, R-245fa. Next the conditions in each apparatus were specified as close as possible to the theoretical values. The first conditions set were those for the heat sinks/sources. It was assumed that the pressure for the heat/cooling sources was 3 bar. This was chosen at random and has almost no effect on the operation/performance of the cycle. In order to model the 9 MMBTU/hr of heat input at 200 degrees Fahrenheit, heat source eight

was given a pressure of 3 bar (43.5 psia), a temperature of 95 degrees Celsius (203 °F), and a mass flow rate of 62.5 kg/s (137.8 lbm/s).The mass flow rate was originally set to a value that corresponded with 9 MMBTU/hr but then was changed in order to force the cycle to produce the desired power. This was necessary because the flow rate of the refrigerant cannot be increased any other way. Source 6 was given a temperature of 15 degrees Celsius (59 °F), a pressure of 3 bar (43.5 psia), and a mass flow rate of 60 kg/s (132.3 lbm/s). The sinks, apparatuses 9 and 7, do not have anything specified except the pressure from the source. Cycle-Tempo calculates the temperature drop and mass flow into the sinks.

The next apparatuses set were the actual components of the ORC. The boiler, which is modeled as a simple heat exchanger, was set to have a pressure of 10 bars on the refrigerant side and a pressure of 3 bars on the waterside. The outlet temperature on the refrigerant side was set to 91.25 degrees Celsius (196.25 °F). The turbine was set to have a pressure of 10 bars and an estimated mechanical efficiency of 80% with an isentropic efficiency of 70%. The generator was specified to have an estimated efficiency of 95%. Cycle-Tempo calculates the actual efficiency of these devices but an initial guess is required to perform the iterations. The condenser was set to have an inlet pressure of 2.79 bars on the refrigerant side and it was specified that the refrigerant would have to a quality of zero when it exits the condenser. Lastly the pump's operating conditions were set to complete the cycle. The pump was specified to increase the pressure of the refrigerant from 2.79 bars to 10 bars. The outlet temperature of the pump was also specified to be 46.29 degrees Celsius (115.32 °F). Now that the cycle's state points were set Cycle-Tempo was run and the results were calculated.

The output for Cycle-Tempo is a text file that contains the calculated mass flow rates for the refrigerant as well as an energy balance for each apparatus and the calculated efficiencies of each apparatus. The table below shows the power consumed by the pump and produced by the generator.

Table 2.5: System Efficiencies

System Efficiencies				
	No.	Apparatus	Energy	Totals
			[kW]	[kW]
Delivered	1	Generator	260.22	
gross power				260.22
Aux. power	1	Pump	60.48	
consumption				60.48
Delivered				
net power				199.73

Table 2.5 above shows that the generator produces about 260 kW and the pump consumes about 60 kW of power. Since the ideal cycle previously analyzed produced 300 kW the value of 260 kW seems reasonable to account for losses within the system and irreversibilities. The pump work calculated by Cycle-Tempo was found to be about 60 kW whereas the ideal pump work was calculated to be about 40 kW. The difference in pump work is due to the fact that the pump is assumed to be ideal in the first analysis and the Cycle-Tempo analysis takes into account the efficiency of the pump. Although Table 2.1 shows that the net power is about 200 kW this is incorrect because if this cycle was at a facility the facility would use the power they already have to power the pump. Table 2.6 shows the results of the energy balance performed on the cycle.

Table 2.6: Energy Balance

Energy Balance				
No.	Name	Energy loss (enthalpy)	Energy loss (HHV)	Energy loss (LHV)
		[kW]	[kW]	[kW]
3	Turbine	265.5	265.5	265.5
4	Condenser	0	0	0
2	Heat Exchgr.	0	0	0
1	Pump	-53.43	-53.43	-53.43
6	Sink/Source	-3796.15	2499.6	149001.94
7	Sink/Source	6306.8	11.04	-146491.3
8	Sink/Source	-24886.42	-18328.34	134278.27
9	Sink/Source	22163.71	15605.63	-137000.97
	Total:	0	0	0

The heat exchangers do not consume any energy since they simply transfer the heat from one fluid to the other. The first law of thermodynamics is satisfied since the overall balance of energy within the cycle is zero. The first column, in the table above, corresponds to the energy based on enthalpy values whereas the next two columns calculate the energy based on the higher heating and lower heating values. The heat loss from the sources/sinks are based on the waterside heat transfer not the refrigerant side, which is why the values are so high since the mass flow rate of the water is higher than the theoretical input. Table 2.7 below shows the data for each pipe in the Cycle-Tempo calculation.

Table 2.7: Data for all pipes

Data for all pipes									
Pipe	Medium	Mass flow	Mole flow	Volume flow	Pressure	Temperature	Enthalpy	Entropy	Quality
no.		[kg/s]	[kmol/s]	[m3/s]	[bar]	[°C]	[kJ/kg]	[kJ/kg.K]	[%]
1	StanMix 1	12.878	0.096	0.0098265	2.79	43.3	-168.78	-0.5908	0
				0.0098265	2.79	43.3	-168.78	-0.5908	0
2	StanMix 1	12.878	0.096	0.0098681	10	46.3	-164.63	-0.5795	0
				0.0098681	10	46.3	-164.63	-0.5795	0
3	StanMix 1	12.878	0.096	0.23278	10	91.25	46.8	0.014	100
				0.23278	10	91.25	46.8	0.014	100
4	StanMix 1	12.878	0.096	0.88718	2.79	58.92	26.18	0.0242	100
				0.88718	2.79	58.92	26.18	0.0242	100
7	WATERSTM	60	3.331	0.060048	3	15	63.27	0.2244	0
				0.060048	3	15	63.27	0.2244	0
8	WATERSTM	60	3.331	0.060172	3	25	105.11	0.3672	0
				0.060172	3	25	105.11	0.3672	0
9	WATERSTM	62.5	3.469	0.06497	3	95	398.18	1.25	0
				0.06497	3	95	398.18	1.25	0
10	WATERSTM	62.5	3.469	0.064503	3	84.64	354.62	1.13	0
				0.064503	3	84.64	354.62	1.13	0

The table above shows the data for each pipe within the cycle. There are two rows for each pipe, the first row corresponds to the inlet of that pipe and the second row is the outlet of the pipe. The fluid called StanMix one is really R-245fa but it is found in the StanMix library which is why that title is displayed. No loses in the pipes were calculated since the values on the inlet rows are the same as the values on the outlet rows. The values of temperature, pressure, and enthalpy appear to be similar to those of the ideal cycle but the biggest difference between the ideal and actual cycles is the flow rate that Cycle-Tempo calculated. The ideal cycle had a mass flow rate of about 27 kg/s whereas the Cycle-Tempo flow rate was about 13 kg/s. Since the flow rate of the refrigerant is about half of the ideal value and cannot be changed the flow rate of the water for cooling and heating had to be increased to its value of 60 kg/s in order to force the cycle to produce the desired amount of power. Even though the flow rate of the Cycle-Tempo cycle is half of the ideal value the flow rate of the heating and cooling water had to be about 10 times greater than desired flow rate for 9 MMBTU/hr.

The efficiencies of the pump, generator, and turbine were calculated to be 88%, 99%, and 86% respectively. The pump and turbine efficiencies seem to be reasonable but the generator efficiency seems to be high. Not sure why this is or how to force Cycle-Tempo to lower this. The estimated efficiency of the generator was changed multiple times but had no effect on decreasing the calculated efficiency of the generator. The last results calculated by Cycle-Tempo are those for the heat exchanging equipment and can be seen below in Table 2.8.

Table 2.8: Heat Exchanging Equipment

Heat Exchanging Equipment				
App.	Name	Low end temp diff.	High end temp diff.	Transmitted heat flow
no.		[K]	[K]	[kW]
4	Condenser	28.3	18.3	2510.64
2	Heat Exchgr.	38.34	3.75	2722.71

The temperature differences on the condenser and boiler, a.k.a. heat exchanger, correspond to the values calculated in the ideal analysis. The low end of each apparatus corresponds to the refrigerant side of the heat exchangers and the high end corresponds to the waterside. The transmitted heat flow for the condenser was calculated to be about 2510 kW whereas the calculated value of the heat rejected in the ideal cycle was approximately 2380 kW. This difference in values corresponds to about a 5% difference. The values should be very close to each other and the difference is assumed to be the fact that two different programs were used to evaluate the properties of the working fluid and these two programs might slightly differ in enthalpy values. The heat flow is calculated only on the enthalpy values of the refrigerant and does not take into account the flow rate from the heat sinks/sources. The heat input flow was calculated to be about 2722 kW in Cycle-Tempo and was found to be 2637 kW in the ideal analysis. This difference is about 3% increase in the heat input. This again is assumed to be due to the fact that two programs were used to evaluate the properties and their values might be based off of different reference points.

The ideal theoretical analysis of the ORC modeled in Cycle-Tempo was assumed to produce 300 kW of electricity, had a mass flow rate of 27.8 lbm/s, had a heat input of 9 MMBTU/hr,

and was found to have a thermal efficiency of about 9.8%. The work input was found to be 0.14 MMBTU/hr and the heat rejected was found to be 8.12 MMBTU/hr. The Cycle-Tempo analysis showed that the cycle could produce about 260 kW, had a mass flow rate of about 13 kg/s, had a heat input of 9.3 MMBTU/hr, a thermal efficiency of about 7.8%. The work input was found to be 0.2 MMBTU/hr and the heat rejected was found to be about 8.5 MMBTU/hr. The thermal efficiency of the cycle is lower since the cycle is not treated as an ideal cycle.

In order to attempt to push the cycle toward its ideal limits a recuperator heat exchanger was added to the cycle. The recuperator heat exchanger is added between the pump and the boiler and is used to take some of the heat out of the refrigerant before it is sent to the condenser and use this heat to preheat the refrigerant before it enters the boiler. The recuperator should increase the efficiency of the cycle but it also increases the cost of the ORC. Figure 2.12 below shows the Cycle-Tempo model of an ORC with a recuperator heat exchanger.

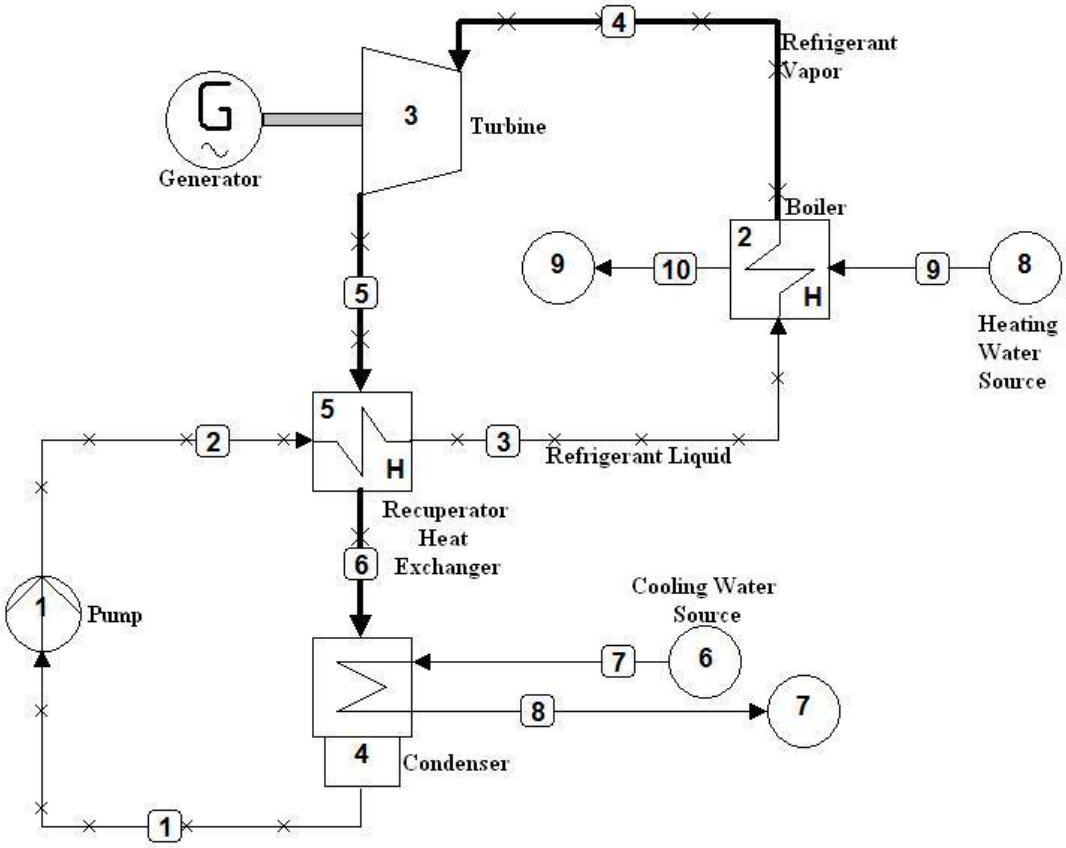

Figure 2.9: Cycle-Tempo ORC with Recuperator

The cycle looks exactly the same as the previous model except for the heat exchanger placed in the middle of the picture, apparatus 5, which connects the turbine to the condenser and the pump to the boiler. The same analysis as the previous cycle was performed on this model. No values were altered between the cycles except for the addition of the recuperator. It was assumed, based on manufacturer's recommendations that the recuperator could increase the temperature of the refrigerant by 10 degrees Celsius. The temperature leaving the turbine is 58C and superheated whereas the temperature leaving the pump is 43C. This 10C rise in temperature across the recuperator corresponds to an 80% efficient heat exchanger. Since the

recuperator is a 100% efficient all the heat is transferred between the fluids and not heat is lost to the surroundings. The connections and the apparatus types are the same as in the previous analysis as well. The system efficiencies for the cycle with a recuperator can be seen below in Table 2.9.

Table 2.9: System Efficiencies for Recuperator Cycle

System Efficiencies				
	No.	Apparatus	Energy	Totals
			[kW]	[kW]
Delivered	1	Generator	273.34	
gross power				273.3
Aux. power	5	Pump	63.34	
consumption				63.34
Delivered				
net power				210

The generator produced about 273 kW and the pump consumed about 63 kW. With the recuperator the generator can produce about 13 more kW than the cycle without. The pump also consumes more power with the addition of the heat exchanger but it only consumes about 3 more kW's than without the recuperator. The increase in pump work is due to an increase in the optimum mass flow rate calculated by Cycle-Tempo. Even though the recuperator increases the work input to the cycle the overall increase in the amount of power produced by the generator is greater than the increase in the power consumed by the pump. This means that the recuperator is a great addition to the cycle to increase the power produced. The next values found from Cycle-Tempo are the completed energy balance for the cycle. These results are shown in Table 2.10.

Table 2.10: Energy Balance for Recuperator Cycle

Energy Balance				
No.	Name	Energy loss (enthalpy)	Energy loss (HHV)	Energy loss (LHV)
		[kW]	[kW]	[kW]
1	Turbine	278.89	278.89	278.89
4	Condenser	0	0	0
3	Heat Exchgr.	-59.38	-59.38	-59.38
2	Heat Exchgr.	0	0	0
5	Pump	-56.13	-56.13	-56.13
6	Sink/Source	-3796.15	2499.6	149001.94
7	Sink/Source	6306.8	11.04	-146491.3
8	Sink/Source	-24886.42	-18328.34	134278.27
9	Sink/Source	22212.39	15654.31	-136952.3
	Total:	0	0	0

The energy balance shows that the first law of thermodynamics is satisfied since no energy is created or destroyed. The values for the sinks/sources are almost exactly the same as the previous cycle which was expected. The values for the energy lost by the pump and turbine are slightly higher than the previous values calculated which was also expected. The main advantage of the recuperator will be seen in the heat exchanging equipment and the thermal efficiency. The next values calculated were the data for all pipes and can be seen below in Table 2.11.

Table 2.11: Data for all Pipes with Recuperator

Data for all Pipes									
Pipe no.	Medium	Mass flow [kg/s]	Mole flow [kmol/s]	Volume flow [m3/s]	Pressure [bar]	Temperature [°C]	Enthalpy [kJ/kg]	Entropy [kJ/kg.K]	Quality [%]
1	StanMix 1	13.527	0.101	0.010322	2.79	43.3	-168.78	-0.5908	0
				0.010322	2.79	43.3	-168.78	-0.5908	0
2	StanMix 1	13.527	0.101	0.010366	10	46.3	-164.63	-0.5795	0
				0.010366	10	46.3	-164.63	-0.5795	0
3	StanMix 1	13.527	0.101	0.010654	10	56.3	-150.88	-0.5371	0
				0.010654	10	56.3	-150.88	-0.5371	0
4	StanMix 1	13.527	0.101	0.24452	10	91.25	46.8	0.014	100
				0.24452	10	91.25	46.8	0.014	100
5	StanMix 1	13.527	0.101	0.93193	2.79	58.92	26.18	0.0242	100
				0.93193	2.79	58.92	26.18	0.0242	100
6	StanMix 1	13.527	0.101	0.89736	2.79	48.92	16.82	-0.0045	100
				0.89736	2.79	48.92	16.82	-0.0045	100
7	WATERSTM	60	3.331	0.060048	3	15	63.27	0.2244	0
				0.060048	3	15	63.27	0.2244	0
8	WATERSTM	60	3.331	0.060172	3	25	105.11	0.3672	0
				0.060172	3	25	105.11	0.3672	0
9	WATERSTM	62.5	3.469	0.06497	3	95	398.18	1.25	0
				0.06497	3	95	398.18	1.25	0
10	WATERSTM	62.5	3.469	0.064511	3	84.82	355.4	1.1322	0
				0.064511	3	84.82	355.4	1.1322	0

The results for the recuperator cycle are very similar to those found earlier for the standard ORC. The main changes are that the mass flow rate was increased from 12.9 kg/s to 13.5 kg/s. This increased flow rate explains why the pump consumed more power in this analysis than the previous one. The other main difference is that the recuperator cycle has an added component which increases the temperature at state 2 by 10 degrees Celsius and decreases the temperature at state 4 by 10 degrees Celsius. It is assumed that this heat exchanger is 100% efficient since the 10-degree temperature difference is lost by one stream and recovered by the other stream. The efficiencies of each apparatus were the same as the previous calculation as well. The turbine was found to be 88% efficient, the pump was 86% efficient, and the generator was found to be 99% efficient. Table 2.12 below shows the heat exchanging equipment heat flow rates.

Table 2.12: Heat Exchanging Equipment for Recuperator

Heat Exchanging Equipment				
App.	Name	Low end temperature diff.	High end temperature diff.	Transmitted heat flow
no.		[K]	[K]	[kW]
4	Condenser	28.3	18.3	2510.64
3	Heat Exchgr.	2.62	2.62	186.01
2	Heat Exchgr.	28.53	3.75	2674.03

In the table above the heat exchanger number 3 corresponds to the recuperator and the heat exchanger number 2 corresponds to the boiler. The heat transfer rate for the condenser is the same as the heat transfer for the previous cycle which is expected since the temperature

output of the cycle is the same. The heat transfer rate for the boiler is a little less than the previous case since the recuperator heat exchanger should increase the inlet temperature to the boiler. The boiler heat transfer rate with the recuperator was found to be 9.124 MMBTU/hr. This is closer to the theoretical ideal analysis than the previous analysis.

The ORC with the recuperator produced about 273 kW, had a mass flow rate of 13.5 kg/s, had a heat input of about 9.1 MMBTU/hr, a thermal efficiency of 7.78%. The work input was found to be 0.21 MBTU/hr and the heat rejected was found to be about 8.5 MMBTU/hr. These values are very close to the previous cycle without the recuperator but the thermal efficiency of the recuperator cycle is the same as without the recuperator. This means that if the price of the addition heat exchanger is reasonable then the increase in power is worth adding the recuperator.

CHAPTER 3

3.1 Case Study:

An aggregate manufacturing facility in Virginia is used for the first case study. Aggregate is coarsely ground particulate material used in construction and mainly consists of sand, gravel or crushed stone. In order to remove the water vapor that is contained in the slate and to "pop" the minerals, it is heated in two rotary kilns at about 1800 degrees Fahrenheit. Slate is usually cured for about 30 days to cool and stabilize. The kilns have a baghouse temperature of 365 degrees Fahrenheit. Shown below in Figure 3.1 is the process description for aggregate production from the facility.

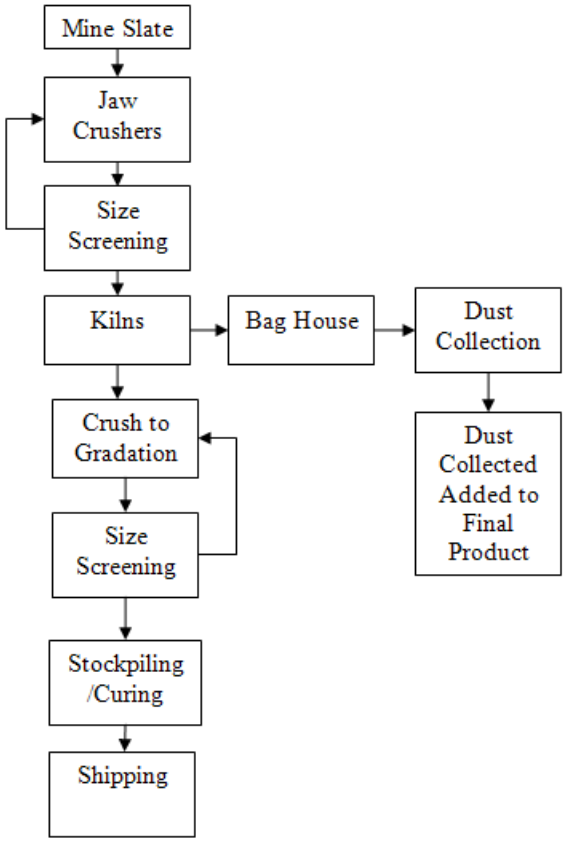

Figure 3.1: Process Flow Diagram

The facility fires the kilns using waste fuel. The main waste fuels used are paint thinner and nail polish thinner. This type of fuel is used mainly because of its cheap price. The facility is a prime candidate for an ORC because of the high mass flow rate of air in the kilns and the high temperature of the kilns. The exhaust air leaving the kiln is processed through a baghouse to collect the debris left in the exhaust and then it is pumped into the atmosphere at a seemingly low temperature, about 365 degrees Fahrenheit which is perfect for utilization in an ORC.

An ORC can take different forms of heat as its input, most of the ORC's for sale use either hot water or heated thermal oil as the input fluid. A liquid input is preferred to a gaseous input because it is easier to ensure that the fluid contains almost no contaminants. This means that the waste heat from the bag house needs to be run through a heat exchanger containing either thermal oil or water before it enters the ORC. Water was chosen in this case due to cost of the thermal oil. Once the water is heated to about 200^0F it enters the evaporator and transfers its heat to the refrigerant in the ORC causing it to change phase and turn into a gas. The hot gas then enters the turbine/generator and produces electricity and the warm water exits the evaporator and returns to a storage tank. The gaseous refrigerant is then pumped through the recuperator heat exchanger and gives some of its heat to the refrigerant that is about to enter the evaporator. The gaseous refrigerant then enters the condenser and is cooled by water until it changes phase and becomes a liquid again. The liquid refrigerant then enters the pump and is pumped through the recuperator heat exchanger then to the evaporator. The

water used to cool the refrigerant is pumped from a nearby river through the condenser and then returns to the river. This process is shown in detail in Figure 3.2 below.

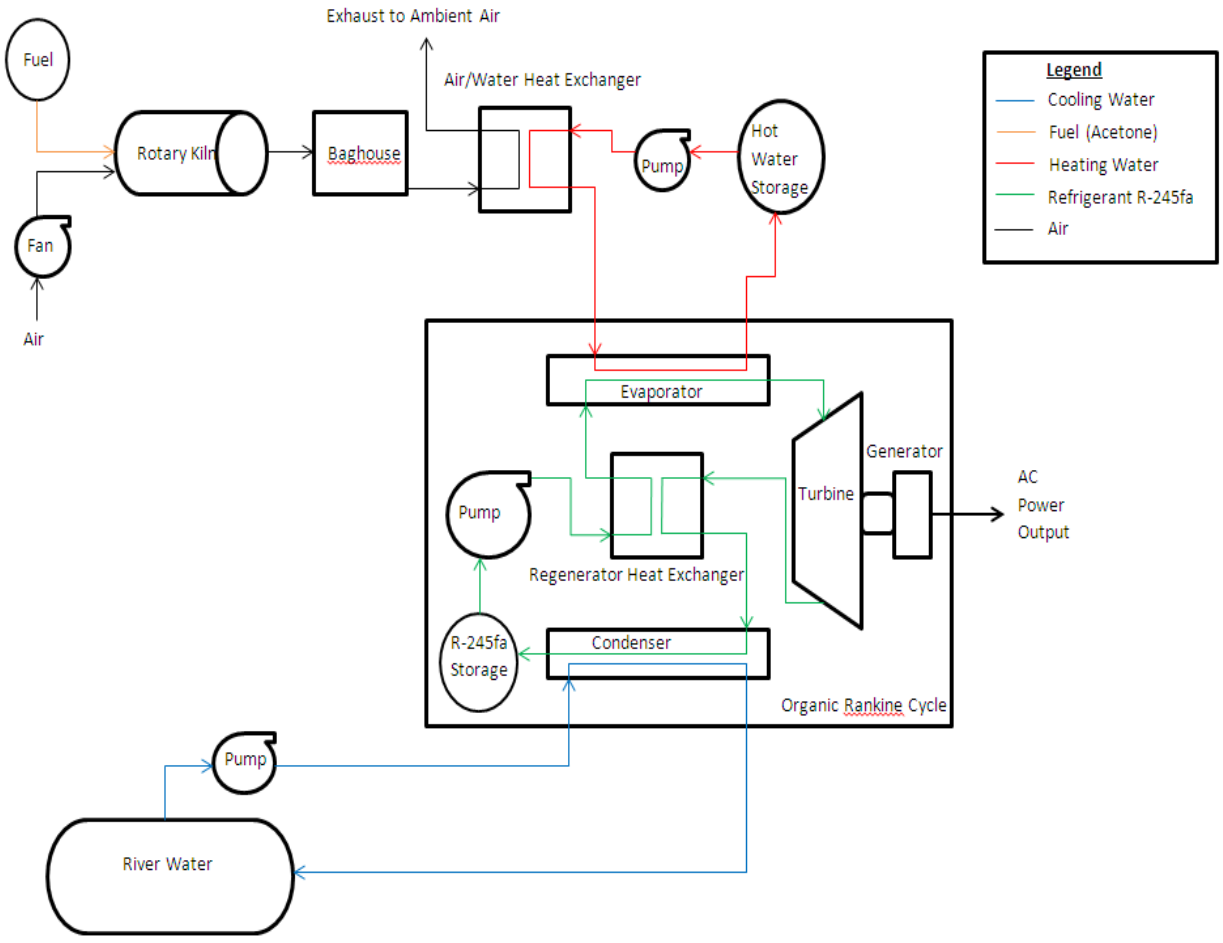

Figure 3.2: ORC Flow Diagram

In order to determine the amount of power that could be produced by utilizing this waste heat the amount of heat being exhausted needed to be determined. First the chemical equation for the combustion of acetone in air was written and balanced stoichiometrically and is shown in equation 3.1.

$$(CH_3)_2CO + 4(O_2 + 3.76N_2) \rightarrow 3CO_2 + 3H_2O + 15.04N_2 \quad (3.1)$$

It can be seen from the above equation that in order for the acetone to be completely burned in air four parts of air are needed for one part of fuel. Since the average fuel flow rate is about 37 lbms of acetone per minute, the theoretical air flow rate is about 84,072 lbms/hr. Note that this is the average mass flow rate of air for stoichiometric conditions (complete combustion) and that the kiln is really going to be firing with more excess air in order to ensure that acetone is completely oxidized and to keep the operating temperature down. Since the ORC's input heat needs to be a maximum of 200 degrees Fahrenheit the amount of heat being transferred from the baghouse to the ORC input can be calculated from the simple heat transfer equation shown below.

$$Q = C_p * m_{dot} * \left(T_{baghouse} - T_{ORC}\right) = 84{,}072\,\frac{lbm}{hr} * \left(0.24\,\frac{BTU}{lb*^0F}\right) * (365 - 200\,^0F) \quad (3.2)$$

Where Q is the amount of heat transferred from the baghouse to the ORC, C_p is the specific heat of air at the average temperature, m_{dot} is the average mass flow rate of air through the kilns, $T_{baghouse}$ is 365 degrees Fahrenheit, and T_{ORC} is 200 degrees Fahrenheit. This will give the maximum heat transfer rate since the temperature difference is maximized but will be evaluated at the theoretical minimum mass flow rate of air. The maximum heat transfer was then determined to be about 3.8 MMBTU/hr for one kiln. Since the facility had two rotary kilns next to each other that were designed to be fired simultaneously the exhaust air could be ducted together to double the mass flow rate of air and ultimately double the rate of heat transferred from the exhaust to the ORC.

It was also investigated how effective a heat exchanger would need to be in order to transfer enough heat to the refrigerant to cause it to change phase to a vapor. This was done by setting the heat transfer for the waterside of the boiler equal to the refrigerant side of the boiler. Figure 3.3 below shows the temperature increase in the working fluid for varying effectiveness of the boiler.

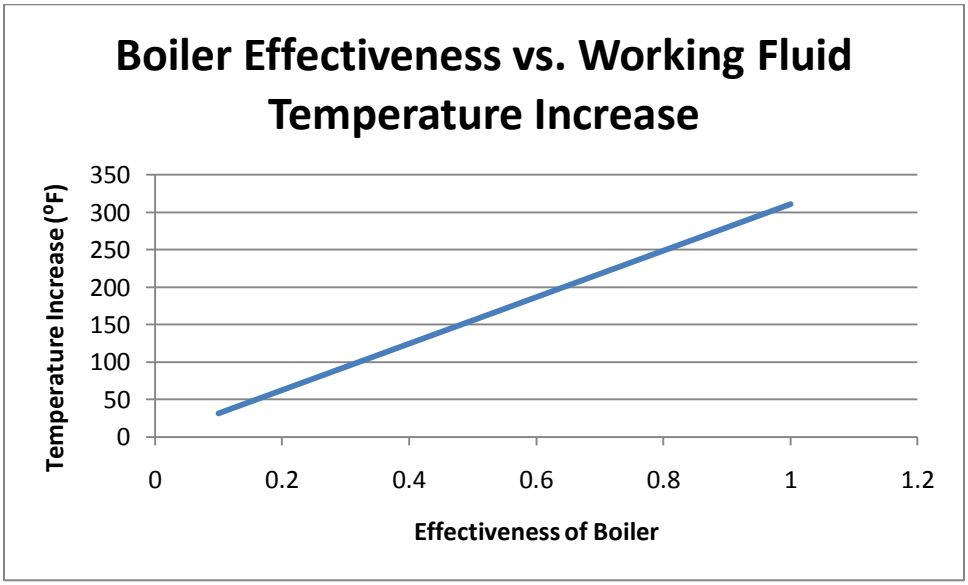

Figure 3.3: Boiler Effectiveness vs. Working Fluid Temperature Increase

It was found that a 50% effective boiler could increase the temperature of the working fluid enough operate an ORC.

According to a turbine manufacturer, in order to find the potential power output from a waste heat application the rate of heat loss should be divided by 35,000 BTU/kWh. The power output for one kiln running an ORC is approximately 108 kW. If the two kilns are ducted together and pumped into an Infinity Turbine ORC the power output would be about 215

kW. Since a 215 kW system could not easily be located, it is best to use a 250 kW system and run it at about 85% of the full load. Since the amount of electricity produced is known the savings from this electricity can be estimated. Since the ORC will produce about 215kW and the price of electricity for the facility is about $0.0549/kWh and $2.13/kW for demand the price of electrical energy saved is about $108,610/yr.

$$Elec\_Cost = 215kW * \frac{\$0.0549}{kWh} * 8736\frac{hr}{yr} + 215kW * \frac{\$2.13}{kW*month} * 12\frac{months}{yr} = \frac{\$108{,}610}{yr} \quad (3.3)$$

There is still one more cost to take into account before calculating the simple payback period. Each pump, the heating loop, cooling loop, and ORC pump requires electrical input to run. The three pumps are estimated to draw a total of about 15kW based on a manufacturer's recommendation which translates to a cost of $7,577/yr.

$$Pump\_Cost = 15kW * \frac{\$0.0549}{kWh} * 8736\frac{hr}{yr} + 15kW * \frac{\$2.13}{kW*month} * 12\frac{months}{yr} = \frac{\$7{,}577}{yr} \quad (3.4)$$

This yields an overall cost savings of about $101,033/yr. The net electrical demand and energy savings are 215 kW and 1,747,200 kWh/yr.

$$Savings = \$108{,}610 - \$7{,}577 = \frac{\$101{,}033}{yr} \quad (3.5)$$

$$Energy = (215kW - 15kW) * \frac{8736hr}{yr} = 1{,}747{,}200\ kWh/yr \quad (3.6)$$

The cost of a 250 kW ORC is $380,000, but this is not a turnkey system which means there are many other costs associated with the ORC. The initial cost does not include shipping either which was estimated to be about $5,000.

The first hidden cost is the location for the ORC. The ORC must be centered on a 20'x10'x6" concrete pad, the cost of concrete is about $750 and the labor and construction cost was estimated to be about $900. The next hidden cost is the refrigerant within the ORC, which costs about $12/lb and requires about 1,500 lb yielding a cost of $18,000. A refrigerant technician is also required to fill the refrigerant and pressurize the system which will cost about $100.

Since the ORC cannot accept the waste heat in the form of a gas it needs to be run through a heat exchanger which will cost approximately $10,000. The water tank needed to store the water used in this heat exchanger is estimated at about $10,000 for a 2,000 gallon tank. Pumps are required to move the water from the storage tank to the heat exchanger as well as from the nearby river to the condenser, which will cost a total of $21,300 for the two pumps. The pumps need to be a 750 gpm and a 1,250 gpm.

The next cost associated with the ORC is the ductwork to connect the exhaust heat to the heat exchanger then to the ORC as well as the cooling water to the ORC, the ductwork was estimated to be about $2,000. A summary of these costs are shown in Table 3.1.

Table 3.1: Summary of Costs

250 kW ORC	$380,000
Shipping Cost	$5,000
Concrete Pad	$1,500
Heat Exchanger	$10,000
R-245fa	$18,000
Refrigerant Tech	$100
Pumps	$21,300
Water Tank	$10,000
Duct Work	$2,000
Fed Grant	$114,000
Tax Cred	$50,000
Subsidy	$6,489
Total	$277,411

Since the ORC uses waste heat, it is classified as an energy efficiency project. Therefore, it qualifies for federal subsidies and tax credits as well as state funded subsidies. The first subsidy available is a federal grant that pays for 30% of the total cost of the ORC which is a savings of $114,000. The next subsidy is a tax credit that is 10% of the total cost but is capped at $200/kW which yields and overall saving of $50,000. There is also another federal subsidy that will pay $0.6/ft^2 of the facility if the implemented technology makes a step towards reducing the electricity use by 50%, which yields a savings of $6,489. The wording of this subsidy is very unclear as to how much energy reduction corresponds to making a step to 50% of the electricity usage. Therefore not every facility may qualify for this subsidy. Other subsidies also exist but the ones listed above were the most applicable and easiest to acquire. After subtracting the subsidies and adding the additional costs, the total cost of

installing the ORC is approximately $277,411. These costs are summarized in Table 3.1 above. With a total cost of $277,411 and a total savings of $101,033/yr the simple payback period is determined to be about 2.8 years.

An economic analysis was also performed for the aggregate facility application of an ORC. Two aspects were investigated under this study. The first was to look at the effect of increasing electricity price on the simple payback period as well as the cost of electricity produced by the ORC and the cost of electricity consumed by the ORC. This was done to investigate the best time to install the ORC if the price of electricity continues to increase. The price of electricity was increased from the current price of $0.0549/kWh by 5% to $0.18/kWh. The results are shown below in Figure 3.4.

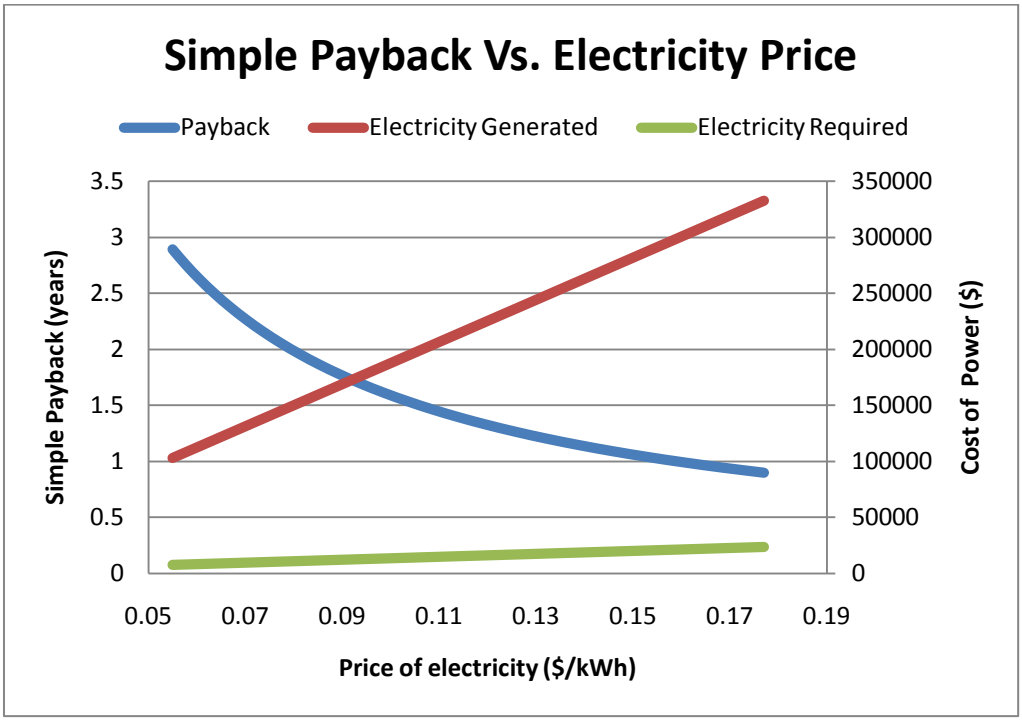

Figure 3.4: Simple Payback and Cost of Power vs. Electricity Price

As can be seen from Figure 3.4 the cost of electricity produced by the ORC and the cost of the electricity consumed by the ORC are linear functions of the price of electricity. Both of these values increase linearly with an increase in the price of electricity. The simple payback period appears to be an exponential decay with the increase in the price of electricity. Since the cost of the ORC does not depend on the price of electricity and the power produced is essentially free power because it was previously wasted to the atmosphere the payback decreases with the increasing price of electricity. If the price of electricity increases to about $0.16/kWh the ORC will pay back in one year. This previous analysis neglects the changing costs of electricity while the ORC is implemented and is meant to serve as a guide of when the ORC should be purchased and installed if the price of electricity were a main factor affecting the implementation of the ORC.

The second economic analysis performed on the facility and the ORC application was assuming that the facility was taking out a loan to pay for the ORC, then the loan payments and interest was calculated for each year. The results are shown below in Table 3.2b and the assumptions in table 3.2a.

Table 3.2a: Loan Assumptions

Loan Principal	$ 280,000.00	Energy Savings (kWh/yr)	1878240
Interest	0.08	Price at t=0 ($/kWh)	$ 0.0549
Loan Term (yr)	20	Savings t=0 ($/yr)	$ 103,115.38
CRF (1/yr)	0.101852209	Escalating at (1/yr)	0.05
Payments ($/yr)	$ 28,518.62		
Tax Bracket	0.305	Personal Discount Rate	0.10

Table 3.2b: Loan Analysis

End of Year	Loan Payment	Interest	Delta Principal	Loan Balance	Tax Savings	Loan Cost	Electric Savings	Net Savings	PV Savings	Cum Pv Savings
0	$0	$0	$0	$280,000	$0	$0	$0	$0	$0	$0
1	$28,519	$22,400	$6,119	$273,881	$6,832	$21,687	$108,271	$86,585	$78,713	$78,713
2	$28,519	$21,911	$6,608	$267,273	$6,683	$21,836	$113,685	$91,849	$75,908	$154,621
3	$28,519	$21,382	$7,137	$260,137	$6,521	$21,997	$119,369	$97,372	$73,157	$227,778
4	$28,519	$20,811	$7,708	$252,429	$6,347	$22,171	$125,337	$103,166	$70,464	$298,242
5	$28,519	$20,194	$8,324	$244,105	$6,159	$22,359	$131,604	$109,245	$67,832	$366,074
6	$28,519	$19,528	$8,990	$235,114	$5,956	$22,562	$138,184	$115,622	$65,266	$431,340
7	$28,519	$18,809	$9,709	$225,405	$5,737	$22,782	$145,094	$122,312	$62,765	$494,105
8	$28,519	$18,032	$10,486	$214,919	$5,500	$23,019	$152,348	$129,330	$60,333	$554,439
9	$28,519	$17,193	$11,325	$203,593	$5,244	$23,275	$159,966	$136,691	$57,970	$612,409
10	$28,519	$16,287	$12,231	$191,362	$4,968	$23,551	$167,964	$144,413	$55,678	$668,087
11	$28,519	$15,309	$13,210	$178,153	$4,669	$23,849	$176,362	$152,513	$53,455	$721,541
12	$28,519	$14,252	$14,266	$163,886	$4,347	$24,172	$185,180	$161,009	$51,302	$772,844
13	$28,519	$13,111	$15,408	$148,478	$3,999	$24,520	$194,439	$169,920	$49,220	$822,063
14	$28,519	$11,878	$16,640	$131,838	$3,623	$24,896	$204,161	$179,266	$47,206	$869,270
15	$28,519	$10,547	$17,972	$113,867	$3,217	$25,302	$214,369	$189,068	$45,261	$914,531
16	$28,519	$9,109	$19,409	$94,457	$2,778	$25,740	$225,088	$199,348	$43,384	$957,915
17	$28,519	$7,557	$20,962	$73,495	$2,305	$26,214	$236,342	$210,128	$41,573	$999,488
18	$28,519	$5,880	$22,639	$50,856	$1,793	$26,725	$248,159	$221,434	$39,827	$1,039,314
19	$28,519	$4,068	$24,450	$26,406	$1,241	$27,278	$260,567	$233,290	$38,145	$1,077,459
20	$28,519	$2,112	$26,406	$0	$644	$27,874	$273,596	$245,721	$36,525	$1,113,984

From Table 3.2a it can be seen that the loan was assumed to be $280,000 since this would cover the total cost of the ORC after rebates and deductions. The interest rate was assumed to be about 8% since this is an average interest rate for loans. The loan was assumed to last over 20 years since the ORC has a lifetime of about 30 years and it was desired to pay off the loan before the life cycle of the ORC was over. It was also assumed that the cost of electricity would increase at 5% per year. The tax bracket was assumed to be 30% and the discount rate was assumed to be 10%. In Table 3.2b, the first column is the number of years passed, the second column is the payment required on the loan which is calculated through the capital recovery factor, the third column is the interest based on the interest rate and the amount of money left in the loan, the fourth column is the remaining balance in the loan, the fifth column is the savings based on the tax bracket, the sixth column is the savings based on the electricity generated and the increasing price in electricity, the seventh column is the net savings, the eighth column is the present value of the savings, and the ninth column is the cumulative savings. The capital recovery factor (CRF) is a function of the discount rate and the number of years of the loan. The CRF is a way of relating the cost of an annuity to the present value of the money obtained from that annuity over the period of time. Table 3.2 shows that under these loan assumptions the overall net present value of the project is about $1,113,985. This means that over the course of the loan the ORC will actually bring in over a million dollars in revenue. It will continue to produce electricity and decrease the facility's demand even after the loan is paid off as well. Since the project has a huge positive net present value it should be implemented immediately to get the most out of the savings.

CHAPTER 4

4.1 Solar Thermal Definition

A solar thermal organic Rankine cycle (STORC) is an organic Rankine cycle that uses water that has been heated by the sun as the heat input for the cycle. The advantage of a STORC is that the heat is free from the sun and it can be used in very rural applications where normal conventional power cannot be used. The main downside from a STORC is the cost of these systems since they require not only a solar collector but also an ORC. Figure 4.1 below shows an example of a STORC. The STORC below uses a system of evacuated tubes as its collector but this may vary from system to system.

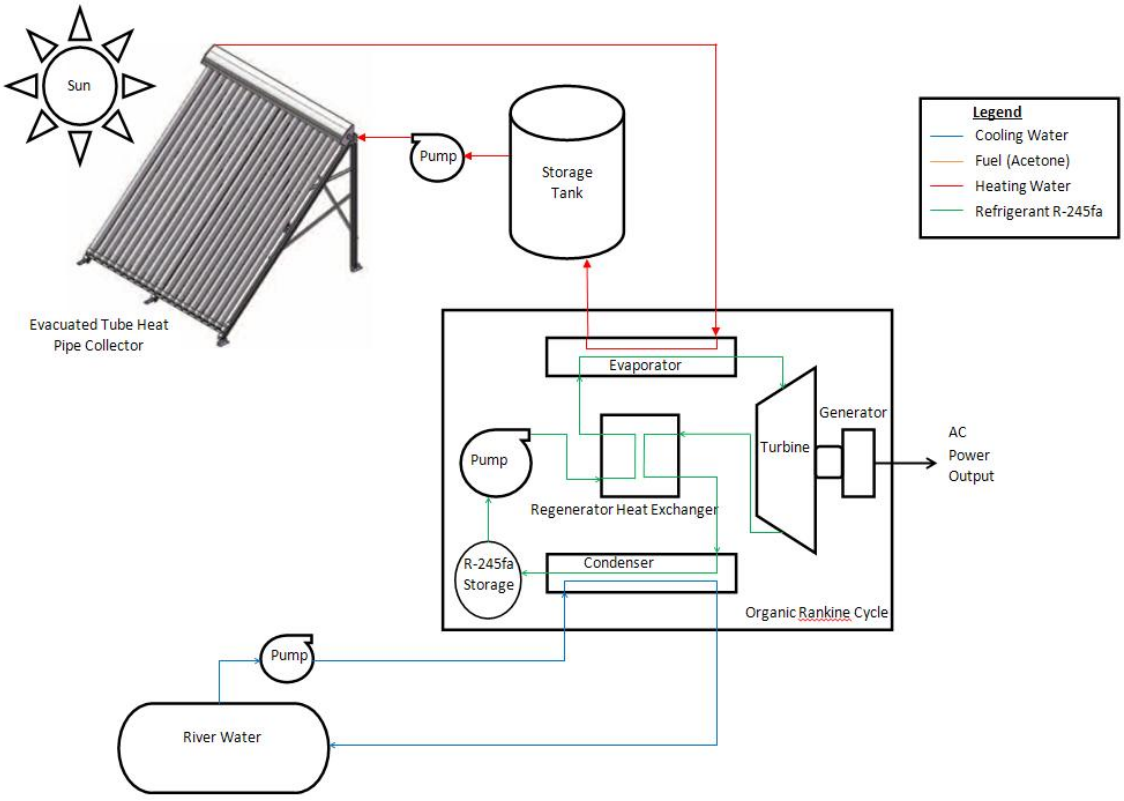

Figure 4.1: Solar Thermal Organic Rankine Cycle Process Diagram

A disadvantage to a STORC is that the sun shines only intermittently therefore thermal storage needs to be added to allow the ORC to produce power all the time. Thermal storage can be very expensive but can increase the capacity factor of a STORC from about 20% to about 70%. Another downside to STORC's is that they require a high mass flow rate of input heat which is usually very hard to obtain because most types of solar thermal collectors require small mass flow rates of water in order to allow the water the heat to the appropriate temperature.

4.2 Collector Types

In order to harness the energy contained in the wavelengths of sunlight a solar collector must be used. A solar thermal collector is a device that captures the wavelengths of the sun and transfers the energy in the sun into heat that can be stored in a fluid. Many types of solar thermal collectors exist and are mainly split into two categories, flat plate and concentrating collectors.

Flat plate collectors can be any type of solar thermal collector that does not concentrate or amplify the sun's rays. These types of collectors can further be broken down into glazed and unglazed collectors. Unglazed collectors are the most common type of collectors. These are usually seen in pool heating applications and are most commonly black plastic tubes on residential roofs. They are called unglazed because there is no glass on the collectors to trap in the sun's rays and prevent them from leaving. The reason these collectors are black is because black materials usually have a higher absorptivity than other colors which means they can absorb more of the sun's rays than other colored materials. These collectors are usually plastic, due to the lightweight and thermal properties of plastic. They also use water as the working fluid since the water is fed directly into the pool. Unglazed collectors usually have high radiation and convective losses due to the absorber being directly out in the atmosphere and not protected by glass or any coatings. They also have a low temperature output due to these high losses and low absorption. This means that they are not ideal choices for power production applications and are mainly used for local heating of water for pools or domestic hot water.

The second type of flat plate collectors are glazed collectors. These are collectors that use glass with selective emissivity to protect the collectors from radiation and convection losses but also to trap in the sun's energy. Figure 4.2 shows an example of the difference between glazed and unglazed collectors.

a) 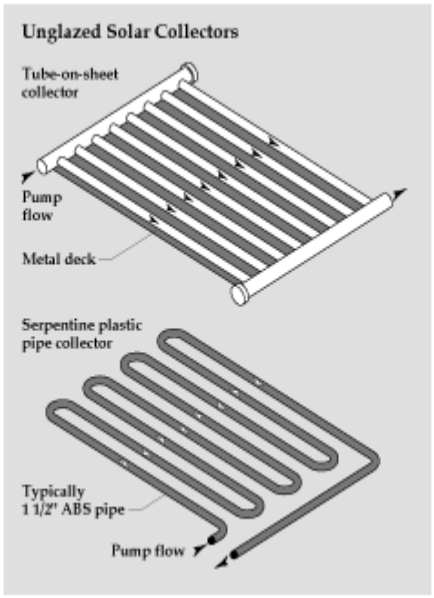

b) 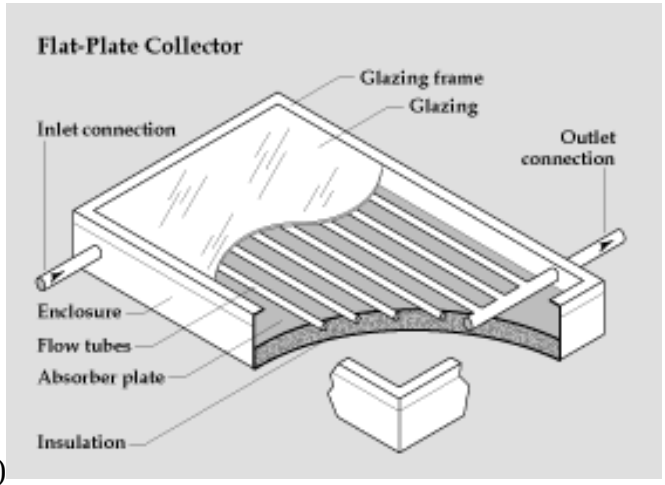

Figure 4.2: a) Unglazed Solar Thermal collectors; b) Glazed Solar Thermal Collectors

The main advantage to using glazed collectors over unglazed collectors is that there is a glass plate that covers the tubes that contain the working fluid. The glass has a selective emissivity which means that the glass allows short wavelengths to pass through the surface of the glass but blocks the longer wavelengths of light from passing through the glass. When the sun's wavelengths pass through the glass the wavelengths becomes longer and get trapped in the glass glazing. The main advantage to this is that fluid in the tubes is subjected to more energy from the sun for a longer period of time. Therefore the collector area can be smaller and the

output temperature from the collector can be higher. The glass glazing also adds a protective layer from the environment. Therefore the losses due to convection and radiation are much less. Glazed collectors can produce higher temperature fluids but are still not widely used in power production cycles. Glazed collectors are mainly used as domestic hot water or pool heating and are commercially available in many sizes and temperature ranges.

The next type of flat plate collectors are not actually flat but are still analyzed the same way so they are often thrown in the same category. These collectors are known as evacuated tube collectors or ETC's. Figure 4.3 below shows an example of these collectors and a brief explanation of how they work.

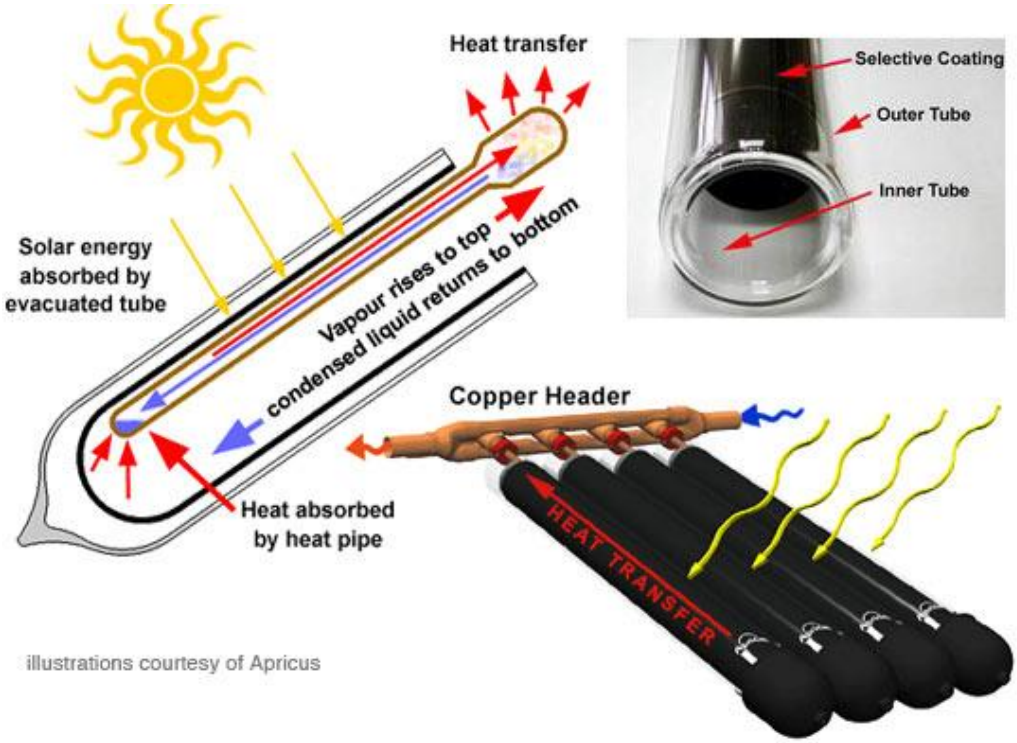

Figure 4.3: Evacuated Tube Collectors

ETC's contain an outer tube, then a vacuum, then an inner tube, then a heat pipe. The outer and inner tubes are separated by a vacuum to reduce the heat loss from the collector since very little heat is transferred through the vacuum. Each one of these tubes is connected in series by a main header. Evacuated tubes are made of two or three different pipes concentrically aligned within each other. The outer most tube is usually glass that is lined with a type of selective coating, usually bromide. This coating is installed to add to the selective emissivity as well as to guarantee the vacuum is held between the pipes. The heat from the sun is trapped in the inner tube by the vacuum and causes the fluid in the heat pipe to evaporate and flow to the top of the header where water flows across the header and causes the fluid to condense and flow back to the bottom of the ETC where it is heated by the sun and the process repeats itself. The fluid in the heat pipe is usually glycol since it has a low freezing point and a low boiling point. ETC's have many advantages over flat plate collectors. ETC's can produce water at an almost constant temperature throughout the entire year because of their high heat absorption and low heat loss coefficient whereas flat plate collectors' performance is greatly affected by the ambient temperature of its environment due to their high losses.

The last type of solar thermal collectors is concentrating arrays. These are devices that concentrate and amplify the sun's rays in order to produce higher output temperatures and can be used in direct steam generation or power production cycles. Many types of concentrators exist; the most common types are parabolic troughs, parabolic dishes, Fresnel collectors, and heliostat field collectors. All of these types of collectors can be seen in Figure 4.4.

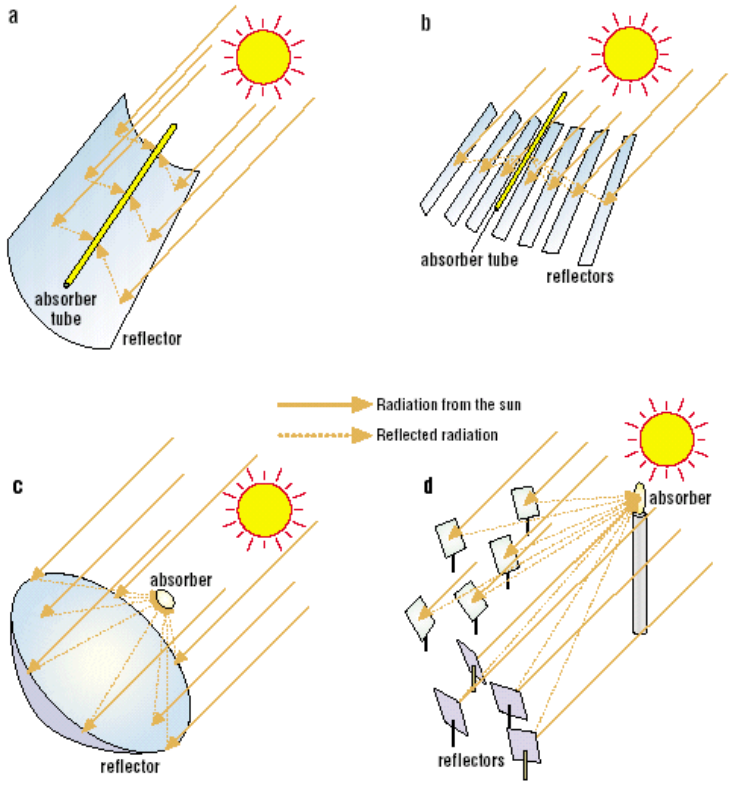

Figure 4.4: Concentrating Collectors; a) parabolic trough, b) Fresnel, c) parabolic dish, d) heliostat collectors

Parabolic troughs are the most common type of concentrators and are widely used in large-scale solar power production applications. Parabolic troughs are shown in Figure 4.4 a). Parabolic troughs work by capturing the direct beam radiation from the sun and focusing it at the focal point of the parabola due to the physical shape of the parabola. At the focal point a glass tube that contains the working fluid is located. The sun's rays then hit this glass tube and cause the working fluid to absorb the sun's energy and heat up the fluid. Parabolic troughs can achieve temperatures up to about 400 degrees Celsius. This hot fluid can then be pumped to multiple end uses. Some of these devices directly produce steam while others will

send the hot water to a heat exchanger to transfer the energy to another end use. Since parabolic troughs only absorb direct beam radiation from the sun, their main downside is that they must follow the sun throughout the entire day. This means that they require a tracking system which requires some form of electrical input before power is produced by the system. This means that most of these systems must be grid connected and may not be ideal for rural applications. They can also be oriented in multiple ways. Either they are oriented with their axes north south and they track from east to west or they are aligned east to west and track north to south. The latter choice is the best option for a constant performance throughout the year.

The next type of collector is the parabolic dish collector which works off a very similar principle as the parabolic troughs. Parabolic dishes can be seen in Figure 4.4 c). Since parabolic dishes also require direct beam radiation to work properly they have to track the sun as well, but since they don't have uniaxial symmetry, like the parabolic troughs, they have to track the sun on both axes and point directly at the sun at all times. One advantage to parabolic dishes is that the heat generated by concentrating the rays can be used directly at the receiver as opposed to parabolic troughs which must heat a fluid then use that fluid to transmit heat energy somewhere else. Parabolic dishes often have a Stirling engine that is attached to the dish which can be run from the concentrated heat and produce electricity on site. Parabolic dishes can have concentration ratios of up to 2000 and produce temperature greater than 1500 degrees Celsius.

Fresnel collectors are seen in Figure 4.4 b) and are composed of many Fresnel lenses that

focus the sun's rays into a central receiver. These can be thought of as parabolic troughs that are split into many different lenses. The advantage to this type of collector is that they don't have to track the sun but they cannot produce as high of temperatures as parabolic dishes or troughs. These are commercially available but not as widely used as troughs due to cost of the lenses and the amount of land required.

The last type of concentrating solar thermal collectors is heliostat collectors and can be seen in Figure 4.4 d). These are mainly used in large-scale power production facilities. Essentially these are composed of lots of small mirrors that all point at the sun then reflect the sun towards a central receiver, usually on a tower, that can produce steam. These can produce the highest temperature of the collectors and can be used to produce the most energy but are also the most costly form of collectors. These are only used in large-scale commercial facilities.

4.3 Sun's Position

One of the most important factors in any solar project is being able to accurately know where the sun is located and how much insolation is available to be used. In order to accurately do this many models and approximations exist. The one used in this project was based on the methods outlined in "Solar Energy Engineering Processes and Systems" by Dr. Soteris A. Kalogirou. All of the angles and position of the sun are based on apparent solar time (AST). This convention sets solar noon as the time when the sun is due south and is at its highest in the sky throughout the day. This process calculates the theoretical solar geometry angles for every hour of every day of the year. Once the geometry was known the solar insolation was calculated. All the calculations were performed in Matlab due to the large size of the matrices, 365 x 24, required to process the data. The main assumptions made to calculate these values are that the collector will be located in Raleigh, NC and it will be tilted at an angle of 35 degrees relative to the horizon. Another main assumption is that the values are only calculated during the day length, while the sun is above the horizon. The collector will also be facing due south and is a stationary collector, meaning it won't track the sun. The main angles associated with a solar thermal collector are: the incidence angle which is defined as the angle at which the sun's rays are striking the collector, the azimuth angle which is defined as the angle of the sun's rays measured in the horizontal plane from due south, and the altitude angle which is defined as the angle between the sun's rays and the horizontal. The azimuth and altitude angle are independent angles that can be used to define the exact position of the sun. The incidence angle is used to determine how much sun is striking the collector. Each of these angles is plotted below for every hour of the year.

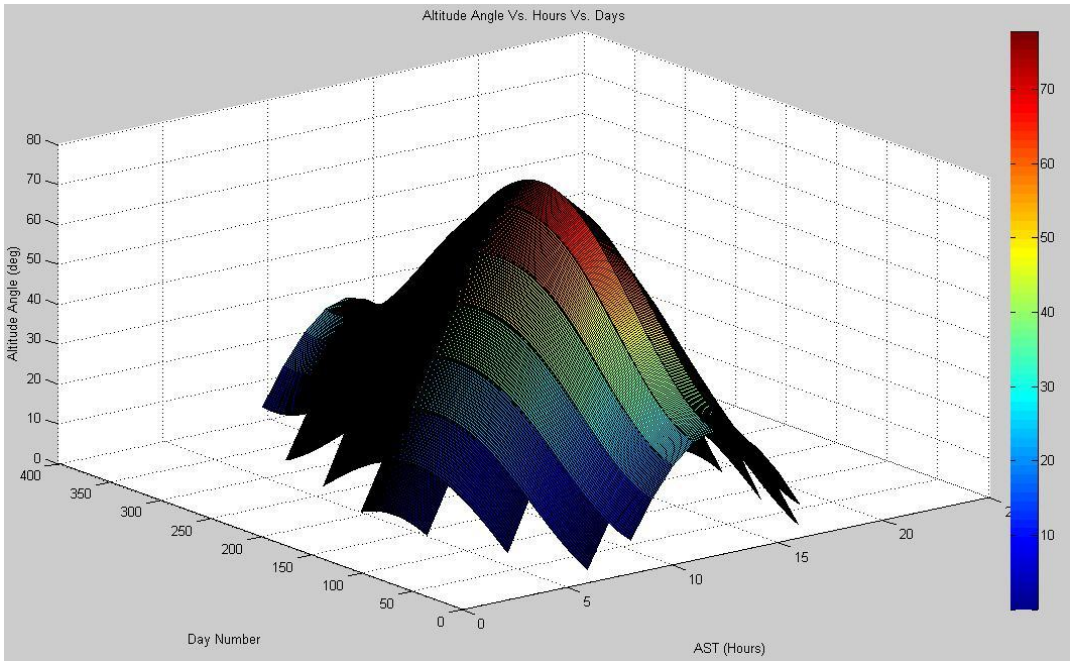

Figure 4.5: Altitude angle vs. Day number vs. AST

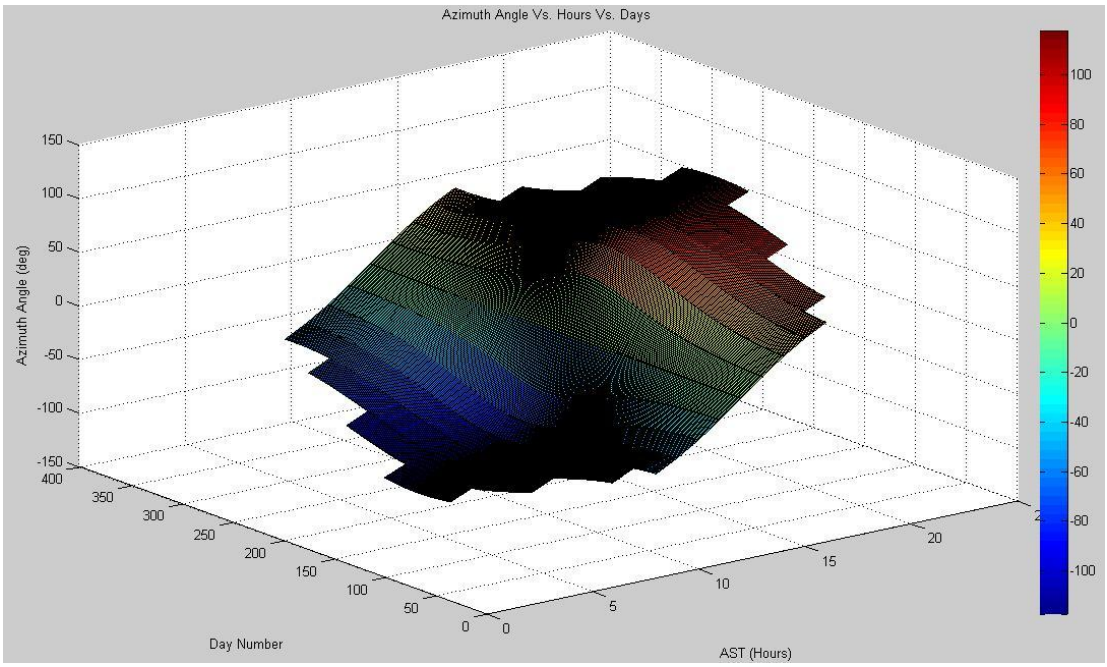

Figure 4.6: Azimuth angle vs. Day number vs. AST

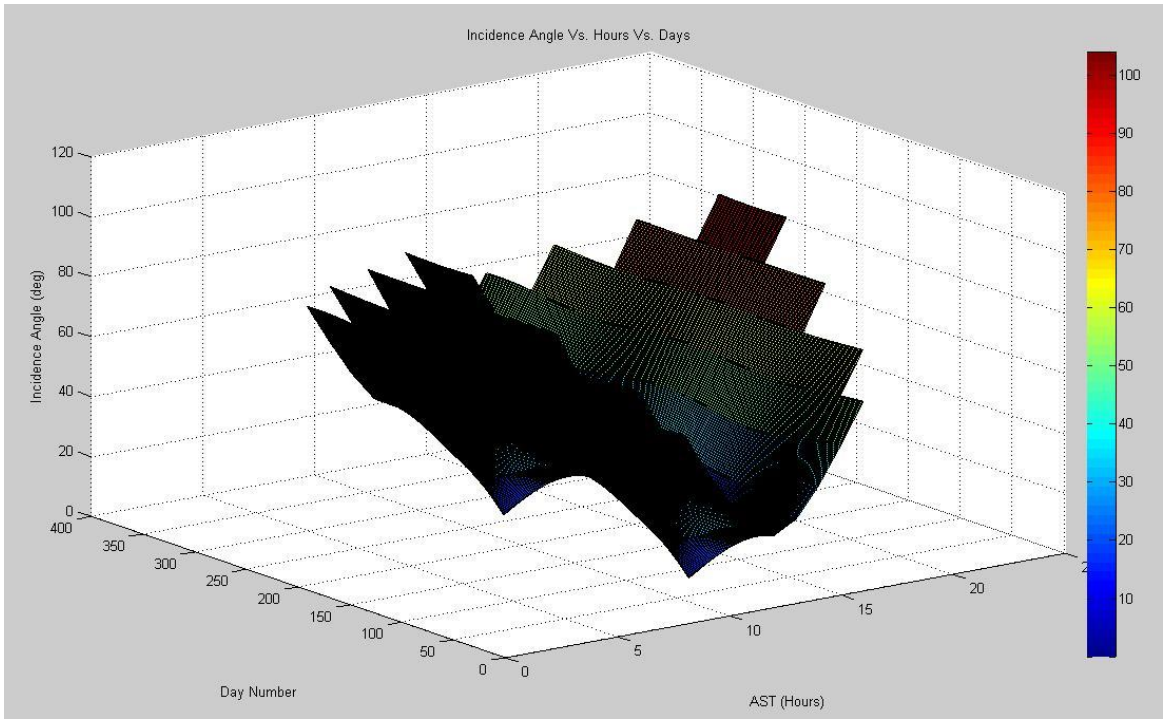

Figure 4.7: Incidence angle vs. Day number vs. AST

In order to calculate these angles the declination angle of the sun was calculated for each day of the year, then the hour angle and day length was calculated for each hour of each day. Once these angles were known the Matlab code was modified to calculate the amount of insolation would be available from the known position of the sun. These values can be seen below.

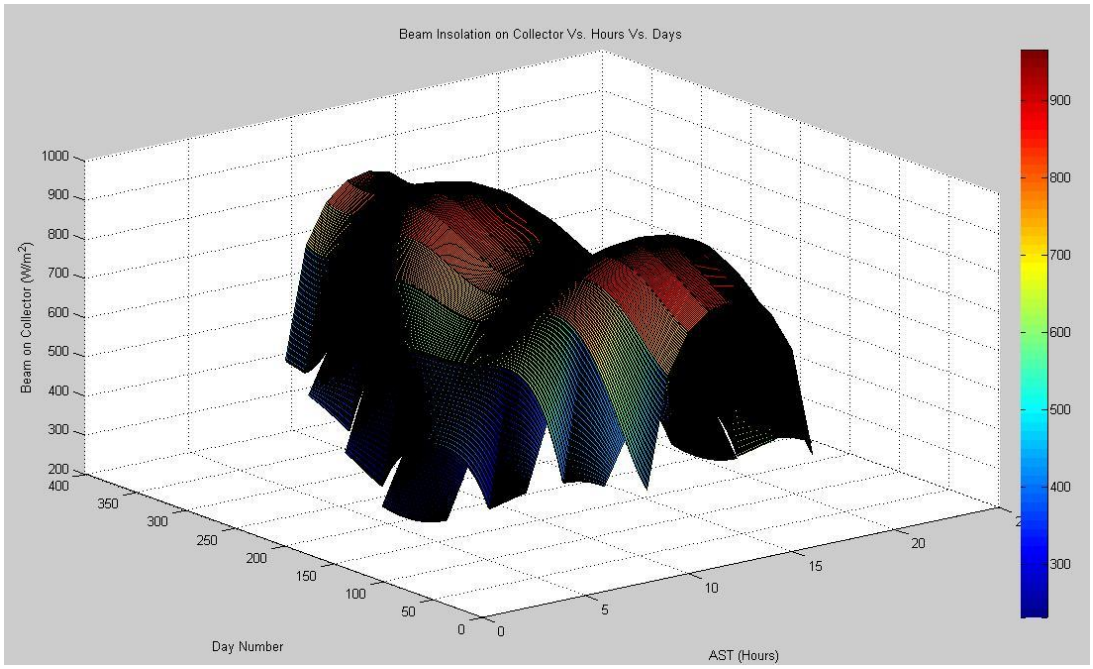

Figure 4.8: Beam Insolation vs. Day number vs. AST

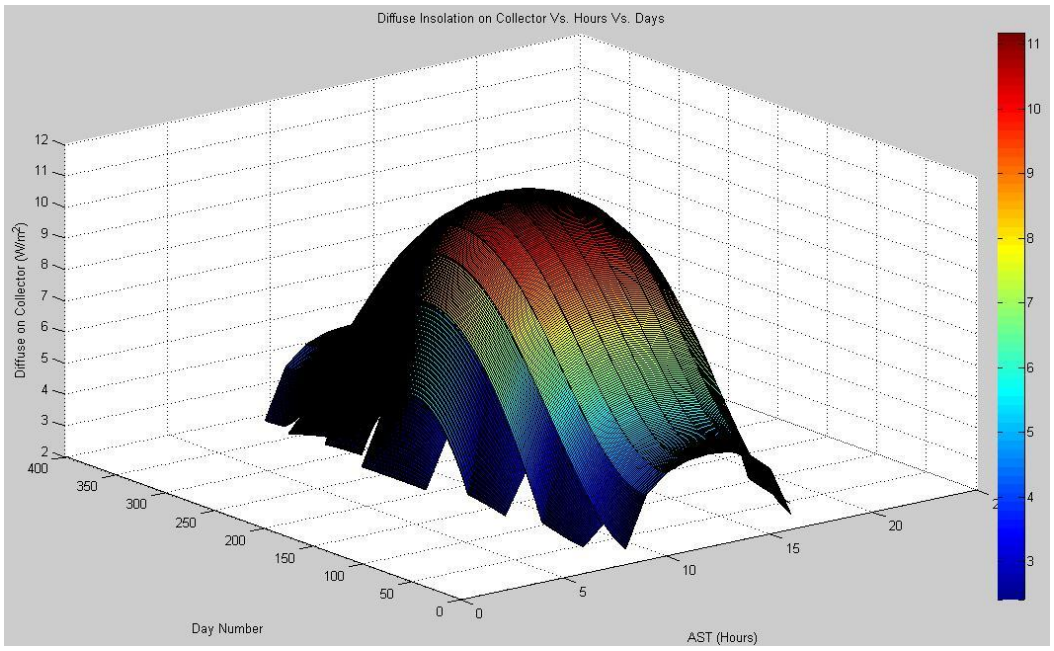

Figure 4.9: Diffuse Insolation vs. Day number vs. AST

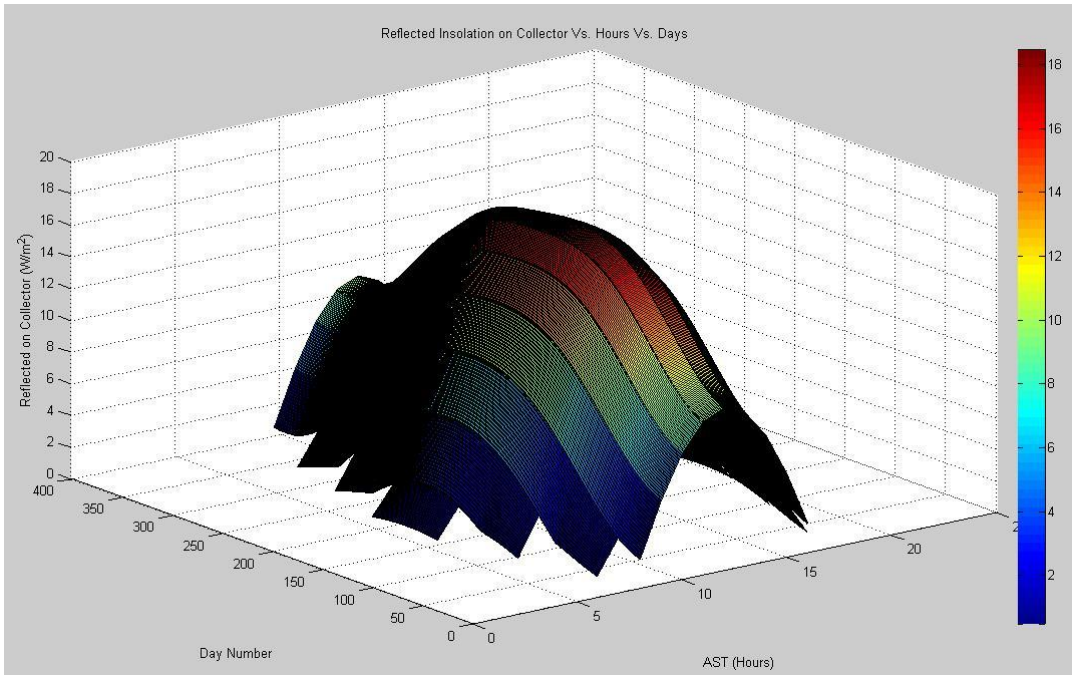

Figure 4.10: Reflected Insolation vs. Day number vs. AST

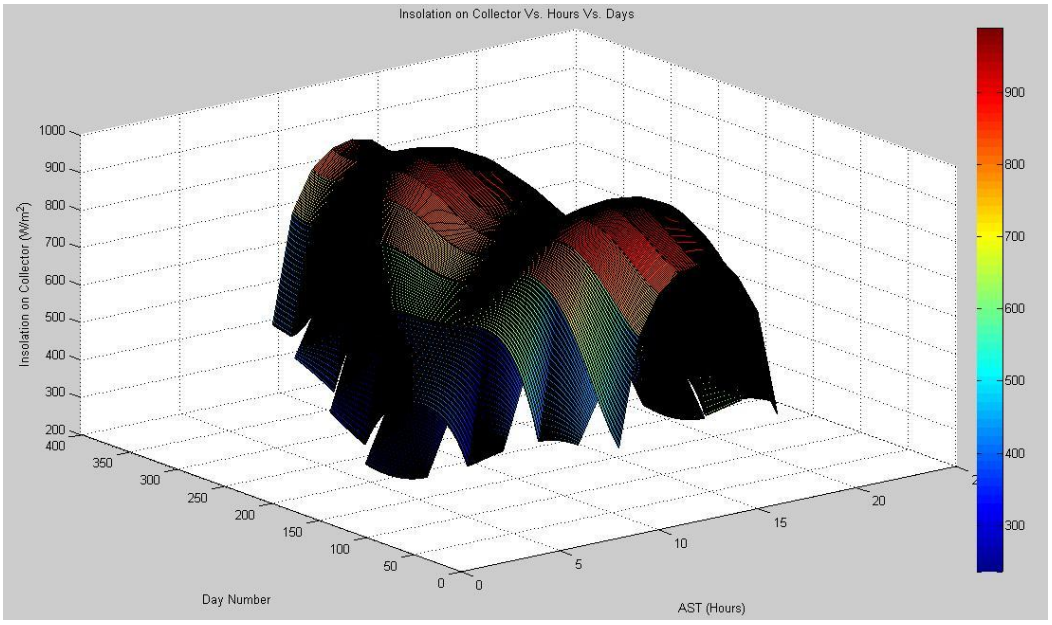

Figure 4.11: Total Insolation on Collector vs. Day number vs. AST

The previous graphs display the expected trends. It was expected that the sun would be highest in the sky close to solar noon. It was also expected that the sun would be higher in the sky during the summer months than the winter months. When the sun is higher in the sky it also emits more insolation which means the collectors can absorb more heat at these times. These insolation values were calculated following the same procedure as above but an air mass correction factor had to be calculated. Since the air mass index can theoretically approach infinity a maximum value was set at 7. This value was chosen because after this threshold the air mass index did not seem to affect the amount of absorbed radiation as much. These values appear to be accurate since the highest amount of total radiation on the collector is less than but close to the maximum theoretical value of 1000 W/m^2.

A main problem with these results is that they do not include cloud cover or shading effects and are only theoretical values. Since there are many problems with these calculated values it was assumed that they would be too inaccurate to be used to calculate actual performance of the STORC. Instead the values used to calculate the performance of the cycle and the actual operating parameters were obtained from NASA's solar and meteorological database and are based on a 22-year average. These values are based on a monthly daily average which means that the value in question was measured for 22 years and the average monthly value was taken to be an average day in that month and is assumed to be an accurate measurement of the value for everyday of that month. It was decided that these values would provide a better actual idea of how well the device would perform since they would include cloud cover and many other variations in solar data.

4.4 ETC STORC Analysis

Solar thermal power plants have been operational in many places in the US since the 1980's. Currently most solar thermal power plants are large-scale power plants that produce over 1 MW of electricity. These plants use parabolic troughs to heat organic based fluids to high temperatures then use the heat from that fluid to create steam and run a traditional Rankine cycle. Since most of these plants still use water as the working fluid in the power production cycle a solar thermal power plant that uses an organic based fluid in the power production cycle was investigated. Multiple types of STORC's were analyzed and compared.

First small-scale applications of STORC's were investigated. These small-scale STORC's were analyzed using evacuated tube collectors as the heat transfer mechanism between the sun and the heat transfer fluid. The working fluid in the collector was water. This type of STORC was investigated due to the relatively low cost of the ETC's and the possibility of being a relatively cheap and widely applicable way to produce power.

The first step in determining the amount of power able to produce by a STORC is to determine how much solar radiation the ETC can absorb. In order to accurately calculate this value many intermediate calculations have to be performed based on the configuration and thermodynamic properties of the collectors. ETC's are stationary collectors and do not track the sun. Therefore a way to model the sun's movement throughout the day was needed. It was determined to look at the changes in incidence angle throughout the day because the incidence angle is a measure of the angle at which the sun strikes the collector. Since it was found that the incidence angle varied from about zero to 90 degrees then back to zero on a

daily basis, from the Matlab model. These calculations were performed for varying incidence angles from 10 to 90 degrees in 10-degree increments. When the sun's rays strike the outer tube of the ETC's the rays are scattered and refracted therefore the actual angle with which the sun's rays strike the heat tube inside the ETC is far different than the original incidence angle. The angle with which the sun's rays strike the heat tube is calculated through Snell's law of refraction. Equation one below shows Snell's law where n is the index of refraction, theta one is the incidence angle, and theta 2 is the incidence angle on the heat tube. The index of refraction is a function of the medium that light is passing through. 1.526 was used for this analysis because light is transferring through glass.

$$n = \frac{\sin \theta 1}{\sin \theta 2} \tag{4.1}$$

Solving this equation for theta 2 yields the angle with which the sun is actually striking the heat tube. However this is very counterintuitive because when theta 1 approaches 90 degrees theta 2 approaches 40 degrees. This ultimately leads to the heat tube absorbing more radiation when the sun is at low angles in the sky rather than directly pointing at the ETC's. This is another reason that the analysis was done for varying incidence angles. In order to calculate the absorbed radiation a value known as tau alpha needed to be calculated for each type of radiation: beam, diffuse, and reflected. Tau alpha is a coefficient that accounts for the radiation that is absorbed by the glass on the collector and not transmitted to the heat pipe.

Now that all these intermediary values have been calculated equation 4.2 can be used to find the amount of radiation absorbed by the ETC. The reflected and diffuse radiation does not

depend on the incidence angle and only on the orientation and properties of ETC's.

$$S = [Ib * Rb * (\tau\alpha)b + Id * (\tau\alpha)d * .5 * (1 + \cos\beta)] + [\rho g * (Ib + Id) * (\tau\alpha)g * .5 * (1 - \cos\beta)] \quad (4.2)$$

In equation 4.2; S is the absorbed radiation, I refers to insolation values, subscripts b, d, and g refer to beam, diffuse, and ground reflected respectively, tau alpha values are transmittance coefficients calculated earlier, Rb is beam radiation coefficient that is determined graphically based on the slope of the collector which accounts for insolation striking a tilted surface, ρg is the assumed value for the ground reflectance (.5 in this case), and β is the slope of the collector with respect to the horizon in degrees. The values for Ib and Id are based on the 22-year average values calculated from NASA's database and are shown in the appendix. After all those variables are taken into account the absorbed radiation can be seen below Figure 4.12.

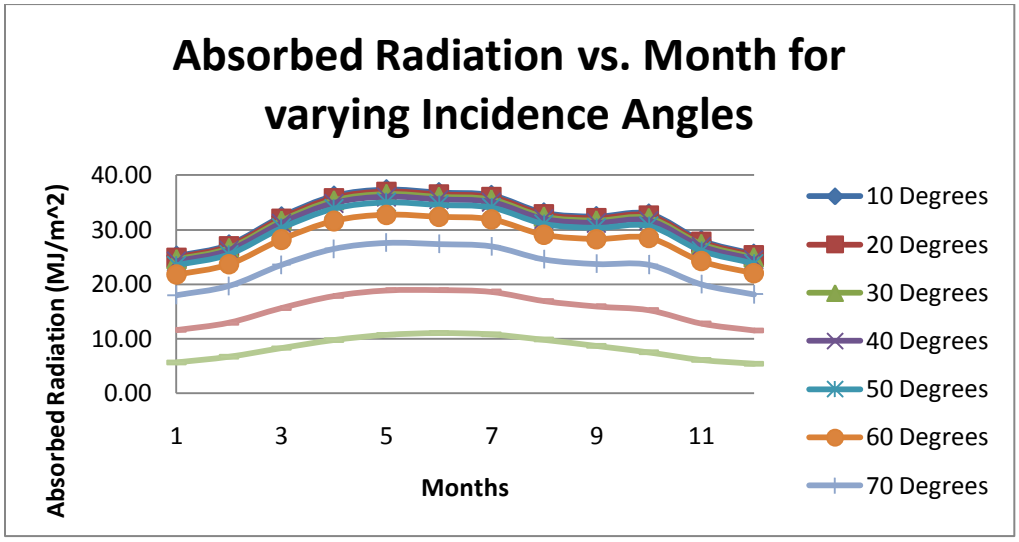

Figure 4.12: Absorbed solar radiation by ETC

The data shown in Figure 4.12 hold true with the expected results of more absorbed radiation in the summer than the winter. The results also show more absorbed radiation at lower incidence angles which is counterintuitive but believed to be accurate. Now that the amount of absorbed radiation was known the next step was to calculate the outlet temperature of the collectors. In order to determine the maximum temperature gain per collector equation 4.3 was used to solve for the temperature difference per unit area of collector.

$$\frac{(Tfo-Tfi)}{Ac} = \frac{Fr*[S-Ul*(Tfi-Ta)]}{mdot*Cp} \tag{4.3}$$

In equation 4.3 above; Tfo is the temperature of the fluid at the outlet of the collector, Tfi is the temperature at the inlet to the ETC, Ta is the ambient air temperature, and Cp is the specific heat of the fluid. The heat removal factor, Fr, was found to be 1.888 from the SRCC rating of the ETC. The overall heat loss coefficient, Ul, was found to be 0.7 W/m^2*^oC from the SRCC rating as well. Ac, the collector area was found from the collector data sheet but was not used in the calculation above. The mass flow rate of the fluid, mdot, was also calculated from the data sheet for the ETC which gave the recommended volumetric flow rate of 0.028 GPM per tube. The value of the solar radiation absorbed by the ETC, S, was previously calculated through equation 4.2. The ambient temperature, Ta, was taken from the 22-year average values for each month. The inlet fluid temperature, Tfi, value was a design set point of 60 degrees Fahrenheit because this is approximately what the temperature of city water would be. Using the assumption of inlet temperature and the aperture area for a collector of 30 tubes from the data sheet, the output temperature from the collectors was able to be calculated. The output temperature was then divided by the desired output temperature

of 200 °F (367 K) to determine the number of tubes required. It was found that 35 tubes could heat the water to the desired temperature, but since the ETC's are only sold in sets of 10 tubes, 40 tubes were used. The mass flow rate was then adjusted to match the recommended flow for 40 tubes and the output temperature was calculated for a 40-tube system. The annual average for varying incidence angles is shown in Table 4.1.

Table 4.1: Outlet Temperature of ETC

Using 40 tubes	Theta	Annual Av
To (K)	10	330.91
	20	330.47
	30	329.95
	40	329.36
	50	328.23
	60	325.50
	70	319.53
	80	309.33
	90	299.80

By looking at the basic equation of heat transfer one can see the temperature output varies linearly with the mass flow rate. This means the mass flow rate has a massive effect on the temperature output of the ETC's. This is a problem for a STORC application because an ORC requires a large amount of heat input but at a relatively low temperature. This means a high mass flow rate is required for ORC's but ETC's are required to have low mass flow rates so the water can completely condense the glycol and absorb all the heat from the sun. A manufacturer has been quoted to say that it requires about 35,000 BTU/h to produce one kW/h from an ORC. The solar thermal system designed above is producing about 10,000 BTU/h. It will take about 208 parallel systems of these 40-tube ETC's to produce about 60

kW. This means that using the ETC's for a residential or small-scale STORC system is completely unfeasible due to the number of ETC's required and the amount of land to place all of these collectors.

4.5 PTC STORC Analysis

The next type of STORC investigated was a large-scale system that uses parabolic trough collectors to heat an organic fluid, Therminol VP-1. The system then uses this hot fluid as the heat input to an ORC. The system was first analyzed without a thermal storage medium in order to investigate the increase in capacity factor with the addition of thermal storage. Although this was never completed because the project was determined to be economically unfeasible before the thermal storage was analyzed. The project was deemed unfeasible because the outlet temperature of the collectors was calculated to be about 700 ^{0}F. Common working fluids in ORC's are not applicable choices for this cycle because 700 ^{0}F is greater than the critical temperature for most of these fluids. Due to the very high outlet temperature a standard steam Rankine cycle would be more feasible to use. This makes sense since most of the SEGS (Solar Electric Generated Steam) plants that are already operational use a standard steam Rankine cycle. The analysis below describes how this outlet temperature was calculated.

The method to analyze concentrating collectors was the same method that is outlined in chapter 3 of [Kalogirou, 2009]. Two types of analysis were performed on the PTC system. The first was an optical analysis that determines the physical characteristics of the PTC. This determines the length and size of the parabolic troughs as well as the optical efficiency. The second analysis performed is a thermal analysis that determines the temperatures of the fluid in the collector, the amount of solar radiation that is absorbed, and the collector efficiency.

The optical analysis begins by defining physical parameters that are essential to the operating

point of the PTC. The first parameter defined was the rim angle, which is the angle with respect to the centerline of the parabola at which the sun strikes the surface of the parabola at the rim. The wider the rim angle corresponds to more sun that the PTC can collect. The rim angle was set to 80^0 for this analysis. In order to verify the accuracy of these results all the physical characteristics were set very close to the SEGS II plant in Arizona. The aperture width was set to 20ft because this is approximately the width of the SEGS plant in English units. The outer diameter of the glass receiver was set to 1 inch. The length of one trough was determined to be 100 ft. Next the latus rectum, focal length, rim radius, and parabolic length were calculated through geometry of a parabola. The focal length and the latus rectum were calculated to be 5.96 ft. The rim radius and parabola length were found to be 10.15 ft and 22.15 ft respectively. Figure 4.13 shows an image of a parabola which defines these quantities.

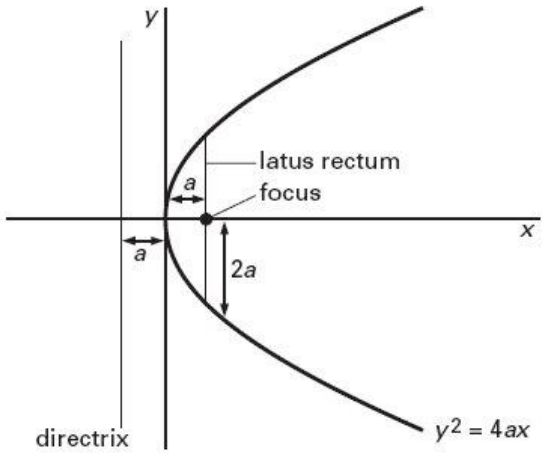

Figure 4.13: Parabola Displaying Focal Length and Latus Rectum

The concentration ratio was calculated trough equation 4.4 below.

$$C = \frac{W_a}{\pi * D} \tag{4.4}$$

The concentration ratio is a measure of how much the collector amplifies the intensity of the sun. It is defined as the ratio of the area of the aperture to the area of the collector. Both the collector and receiver have the same length, therefore it can be eliminated from the equation and just the perimeters of the collector and receiver are used. The concentration ratio was calculated to be about 76. This is very close to the value for SEGS II which has a concentration ratio of 77.

The next values calculated were the area that is lost to end effects of the PTC. Most PTC's have an area at the end of the collector, where beam radiation is reflected but does not strike the receiver. Another part of the area of the collector is shaded by the receiver tube as well. This has to be taken into account with the area lost. The area lost is a function of the focal length of the parabola and the aperture width of it as well. The area lost is used to calculate the optical efficiency of the PTC. The optical efficiency could not be calculated for this analysis because it requires a transient analysis to know how the rim angle varies as the sun moves throughout the day. Therefore the optical efficiency was estimated to be 77% which is the same value as the optical efficiency of the SEGS II plant.

Now that the optical analysis was completed a thermal analysis was performed on the PTC STORC. The main purpose of the thermal analysis is to determine the fluid temperature at the outlet of the PTC. The thermal analysis consists of an iterative process where the

temperature of the fluid is estimated then checked to determine if the first guess is accurate. Since the PTC's track the sun on one axis it was not required to perform the iterations at multiple incidence angles. The first step of the thermal analysis is to calculate the heat loss from the PTC due to convection from the wind and radiation to the ambient temperature. The assumptions required to do this were the inner and outer diameters of the receiver, the emissivity of the receiver and collector, and an estimate for the receiver temperature. The inner diameter was set to 0.75 inches and the emissivity for the collector and receiver were 0.93 and 0.87 respectively. These values were chosen because of the values used on the SEGS II plant. The temperature of the receiver was set to 600 ^{0}F because of an example followed in Kalogirou that had very similar characteristics as the PTC analyzed.

In order to calculate the heat loss from the PTC a guess of the glass temperature had to be made. It was found that the temperature of the glass cover on the PTC is closer to the ambient air temperature than to the temperature of the receiver. Therefore iterations were made at different assumptions of glass temperature. It was first estimated that the glass temperature would be about 1.5 times the ambient air temperature. After following numerous calculations to find the heat loss coefficients for radiation and convection loses from the PTC it was found that a glass temperature of 2.491 times the ambient temperature was the most accurate assumption.

Now that the glass temperature and the heat loss coefficients from the PTC were determined the outlet temperature of the fluid was calculated. Ambient air temperature, wind speeds, and insolation values were determined through NASA's meteorological and solar database that is

based on a 22-year average of data measurements. To calculate the fluid exit temperature equation 4.5 was used to find the useful heat gain from the collector it was then modified to form equation 4.6 and used to calculate the outlet temperature.

$$Q_u = F_R * [S * A_a - A_r * U_l * (T_i - T_a)] \quad (4.5)$$

$$T_o = T_i + \frac{Q_u}{m_{dot} * C_p} \quad (4.6)$$

The heat removal factor, Fr, was found to be about 0.9. The amount of solar insolation, S, in the equation above was found from the 22-year average values from NASA. Aa and Ar are the aperture and receiver areas respectively. The inlet temperature was first assumed to be about 100^0F but was then changed to about 400^0F after talking to an associate at SEGS II. This was done because the fluid is warm when it enters the PTC because it comes from the storage tanks that contain some heat. The specific heat, Cp, was found from Therminol VP-1 thermodynamic properties. The mass flow rate was calculated from a volumetric flow rate of 100 GPM based on SEGS II's flow rate. The useful energy gain was approximately 2000 kW. This leads to an outlet temperature of close to 700 ^{0}F. These results were thought to be inaccurately high when first calculated. After speaking with a SEGS II employee it was determined that they were accurate. The SEGS employee said that the flow rate was 100 GPM and had an outlet temperature at most of 700^0F. Since the temperature was found to be much higher than expected the analysis was stopped here and it was determined that a STORC using PTC's was a poor choice.

4.6 STORC Conclusion

Overall many issues were encountered during the analysis of a STORC. The first issue is the conflicting relationship between temperature and mass flow rate of the ORC's. ORC's can operate at very low temperatures because the working fluids within the cycles have very low boiling temperatures, but in order for an ORC to produce enough power to be economically feasible it has to have a large heat input or a high mass flow rate of the heating fluid. This means that using ETC's in combination with an ORC is a poor choice because ETC's require small mass flow rates of fluid in the collector and would require a large number of collectors to produce the required heat input for an ORC. This means that small-scale at home STORC's are not economically feasible due to the large number of collectors required and the large amount of land required to mount all of the collectors.

The same issue can be used to show that PTC's are not an economical choice for an ORC as well. A PTC using Therminol VP-1 as the heat transfer fluid can obtain a high enough mass flow rate to use an ORC but the outlet temperature of the fluid is close to 700 ^{0}F. With this high of an outlet temperature a standard steam Rankine cycle would be more efficient and cost effective to produce power. Most working fluids used in ORC's have a critical point lower than 700 ^{0}F which means they could not be used at this high of a temperature. Although organic fluids do exist that can operate at these temperatures they are more expensive and less used than water. Therefore it would be better to use a steam cycle.

Possible applications that could support the use of a STORC that were not investigated are solar ponds and direct flash systems. Solar ponds are ponds that contain fresh water and salt

water that are naturally divided due to density differences. Since the fresh water is less dense than the salt water it floats to the surface and acts as an insulator that retains the heat from the sun in the pond. The salt water gets heated through the sun and the fresh water traps the sun's rays in the pond. These ponds can reach temperatures greater than 90 ^{0}C. This is hot enough to power an ORC but it is unsure the size of the pond that would be required to yield a large enough mass flow rate to effectively run a STORC.

The second application not investigated is a direct flash system. This is a system in which a solar collector heats a refrigerant to a desired temperature at a given pressure then the pressure of the fluid is decreased forcing the fluid to expand and flash into a vapor. The vapor is then forced through the turbine generator combination and the standard Rankine cycle is repeated except the flash tank and the solar collector act as the boiler. This might be inefficient though since the pressure is required to decrease before it enters the turbine where the pressure is further decreased.

CHAPTER 5

5.1 Conclusion

Overall an organic Rankine cycle was analyzed in many different applications and aspects. The first analysis was that of a theoretical organic Rankine cycle. This was done in order to compare the thermal efficiency of the cycle at various operating points. It was found that R-245fa is a more efficient working fluid at lower temperatures than R245ca. It was also found that R-123 was more efficient at higher power systems because it had an efficiency over 10% when it the cycle was forced to produce more energy. The boiler pressure and temperature also have a big effect on the efficiency of the cycle. The results vary for the fluids but most of the fluids are more efficient at higher pressures since they are able to produce more power at a higher pressure. The cycle was also analyzed using isentropic efficiencies for the pump and turbine. This showed that the thermal efficiency was linearly proportional to the isentropic efficiency of the turbine.

The mass flow rate also has a very big effect on the ability of an ORC to produce power. This is very evident with the first STORC analyzed. It was found that using ETC's to produce power with an ORC is economically unfeasible. This is because the ETC's require a low mass flow rate through the collector and an ORC requires a high rate of heat input even though it can run at relatively low temperatures. The second solar analysis showed that PTC's produce temperatures that are too high to operate an ORC because the temperatures are greater than the critical point for many organic based fluids.

An ORC was also modeled in a computer program, Cycle-Tempo, in order to see how an

actual cycle could perform. It was found that the actual cycle would produce about 10% less power than theoretically calculated. Cycle-Tempo also calculated the optimum mass flow rate for the working fluid within the ORC to be about half of the theoretical mass flow rate. This required the heat input to be more than doubled in order to force the ORC to produce the desired amount of power.

In the future to continue working on ORC's it is recommended that an ORC connected to a solar pond or to a direct flash system should be investigated. It is also recommended that a transient analysis be performed on an actual ORC in order to see how it performs at various ambient temperatures or various operating conditions. It would also be preferred to collect actual data from an operational ORC to investigate ways the cycle could be made more efficient and to see the actual data from an ORC.

REFERENCES

1. Sloan, M., A.R. Mahoney, T.R. Mancini, G.J. Kolb, D.W. Kearny, C.W. Matthews, V.E. Dudely. United States, Golden, Colorado. *Test Results: SEGS LS-2 Solar Collector*., 2004. Web. 20 Mar 2011.
2. Price, H..,V. Hassani. United States, Golden, Colorado. *Modular Trough Power Plants Cycle Analysis.*, 2004. Web. 20 Mar 2011.
3. Reflective Energies. United States. *The Solar Trough Organic Rankine Electricity System (STORES)-Final Report. Analysis.*, Mar 2006. Web. 15 Mar 2011.
4. **"**Technology Characterization Solar Parabolic Trough**."** SolarPaces. EnergyTechnology Network, 2010. Web. 28 April 2011. <http://www.solarpaces.org/CSP_Technology/csp_technology.htm>.
5. Shroeder, David J., and Leslie, Neil. "Organic Rankine Cycle Working Fluid Considerations for Waste Heat to Power Applications." *ASHRAE Transactions* (2010): Web. 06 Jan 2011.
6. Liu, Bo-Tau, Kuo-Hsiang Chein, and Chi-Chuan Wang. "Effect of Working Fluids on Organic Rankine Cycle for Waste Heat Recovery." 10 Jun 2002. Elsevier. Web. 09 Nov 2010. <www.Elsevier.com/locate/energy>.
7. Maizza, V., and A. Maizza. "Unconventional Working Fluids in Organic Rankine-Cycles for Waste Energy Recovery Systems." 11 Mar 2000. Elsevier. Web. 12 Dec 2010. <www.elsevier.com/locate/apthermeng>.

8. Hung, Tzu-Chen. “Waste Heat Recovery of Organic Rankine Cycles Using Dry Fluids.” 24 Aug 2000. Elsevier. Web. 12 Dec 2010. <www.elsevier.com/locate/apthermeng>.

9. Wei, Donghong, Xuesheng Lu, Zhen Lu, and Jianming Gu. “Performance Analysis and Optimization of Organic Rankine Cycle for Waste Heat Recovery.” 14 Dec 2006. Elsevier. Web. 09 Jan 2010. <www.elsevier.com/locate/enconman>.

10. Quoilin, Sylvain. "Experimental Study and Modeling of a Low Temperature Rankine Cycle for Small Scale Cogeneration." *University of Liege Faculty of Applied Science*. (2007): Print.

11. Quoilin, Sylvain. "An Introduction to Thermodynamics Applied to Organic Rankine Cycles." *University of Liege Faculty of Applied Science*. (2008): Print.

12. Hung, T. C. "A Review of Organic Rankine Cycles for the Recovery of Low-Grade Waste Heat. *“Energy* 22.7 (1997): 1-7. Web. 13 Dec. 2010.

13. Kalogirou, Soteris A. (2009). *Solar energy engineering processes and systems*. New York: Elsevier.

APPENDICES

Appendix A: Sample Theoretical Comparison Spreadsheet

Attempt 1a: (150psi,Tsat) Assumed Qin, Mdot, and Wout

Assumptions

Ideal	s4=s3 P2=P3 P4=P1	
Working Fluid	r245fa	
Units	E	English
M dot	0.1	(10^6)lbm/hr
	27.77777778	lbm/s
W dot gen	0.853035	MMBTU/hr
	250	kW
Q dot in	9	MMBTU/hr
P Max	150	psia
η Isen T	70%	
η Isen P	80%	

	1	2	2a	3	4	4a
s (BTU/lb*R)	0.288558122	0.288558122	0.28843895	0.42860446	0.42860446	0.432842588
h (BTU/lb)	112.5252296	112.7536031	112.69	202.7536031	194.2232531	196.78
ρ (lb/ft^3)	79.89104145	80.01448787	80.03558453	3.615335297	1.178487244	1.149798908
T (°F)	114.8230682	115.3313482	115.1243817	196.2549835	138.8119868	149.532572
P (psia)	51.39455761	150	150	150	51.39455761	51.39455761
Cp (BTU/lb*R)	0.331781091	0.331064878	0.330993998	0.284090355	0.238310308	0.239145132
x (quality)	#Subcooled liquid	#Subcooled liquid	#Subcooled liquid	#Superheated vapor	#Superheated vapor	#Superheated vapor

Energy Balance						**% error**
qin	9	MMBTU/hr	qin	9.006851203	MMBTU/hr	0.076124476
qout	8.169802343	MMBTU/hr	qout	8.425712843	MMBTU/hr	3.132395244
win	0.022837343	MMBTU/hr	win	0.01598614	MMBTU/hr	-30
wout	0.853035	MMBTU/hr	wout	0.5971245	MMBTU/hr	-30
ΔE	0	MMBTU/hr	ΔE	0	MMBTU/hr	
Thermal Efficiency						
η thermal	9.224418414		η thermal	6.4521812		-30.0532466

Attempt 1b: (150psi,Tsat+5) Assumed Qin, Mdot, and Wout

Assumptions

Ideal	s4=s3 P2=P3 P4=P1	
Working Fluid	r245fa	
Units	E	English
M dot	0.1	(10^6)lbm/hr
	27.77777778	lbm/s
W dot gen	0.853035	MMBTU/hr
	250	kW
Q dot in	9	MMBTU/hr
P Max	150	psia
η Isen T	70%	
η Isen P	80%	

RefProp Values

	1	2	2a	3	4	4a
s (BTU/lb*R)	0.291010422	0.291010422	0.290892414	0.430754008	0.430754008	0.434949507
h (BTU/lb)	113.9410868	114.1689062	114.10	204.1689062	195.6385562	198.20
ρ (lb/ft^3)	79.45026922	79.5770564	79.59825255	3.553733454	1.181295444	1.153187089
T (°F)	119.0794564	119.5968505	119.3913054	201.2549835	144.9466698	155.6304729
P (psia)	52.174	150	150	150	52.174	52.174
Cp (BTU/lb*R)	0.333300541	0.332546132	0.33247384	0.282087827	0.239084032	0.239997793
x (quality)	0	0	0	1	1	1

Energy Balance

						% error
qin	9	MMBTU/hr	qin	9.006834581	MMBTU/hr	0.075939793
qout	8.169746938	MMBTU/hr	qout	8.425657438	MMBTU/hr	3.132416487
win	0.022781938	MMBTU/hr	win	0.015947356	MMBTU/hr	-30
wout	0.853035	MMBTU/hr	wout	0.5971245	MMBTU/hr	-30
ΔE	0	MMBTU/hr	ΔE	0	MMBTU/hr	

Thermal Efficiency

η thermal	9.225034025	η thermal	6.452623708	-30.05311752

Assumptions

Working Fluid	r245fa	
Units	E	English
η Isen T	85%	
η Isen P	87%	

RefProp Values

	1	2	2a	3	4	4a
s (BTU/lb*R)	0.298	0.298	0.298	0.429	0.429	0.431
h (BTU/lb)	117.877	118.112	118.147	203.354	195.386	196.582
ρ (lb/ft^3)	78.215					
T (^{o}F)	130.805	131.368	131.472	200.000	145.591	150.353
P (psia)	58.000	157.000	157.000	157.000	58.000	58.000
x (quality)	0.000			1.000	1.048	

sf	0.298	
sg	0.423	
hf	117.877	
hg	191.862	
Q3	#Superheated vapor	

Theoretical			**Actual**		
qin	85.243	BTU/lb	qin	85.208	BTU/lb
qout	77.509	BTU/lb	qout	78.704	BTU/lb
win	0.234	BTU/lb	win	0.276	BTU/lb
wout	7.968	BTU/lb	wout	6.932	BTU/lb
wnet	7.734	BTU/lb	wnet	6.657	BTU/lb

Thermal Efficiency

η thermal	9.073

η thermal	7.633

Carnot Efficiency

η Carnot	10.484

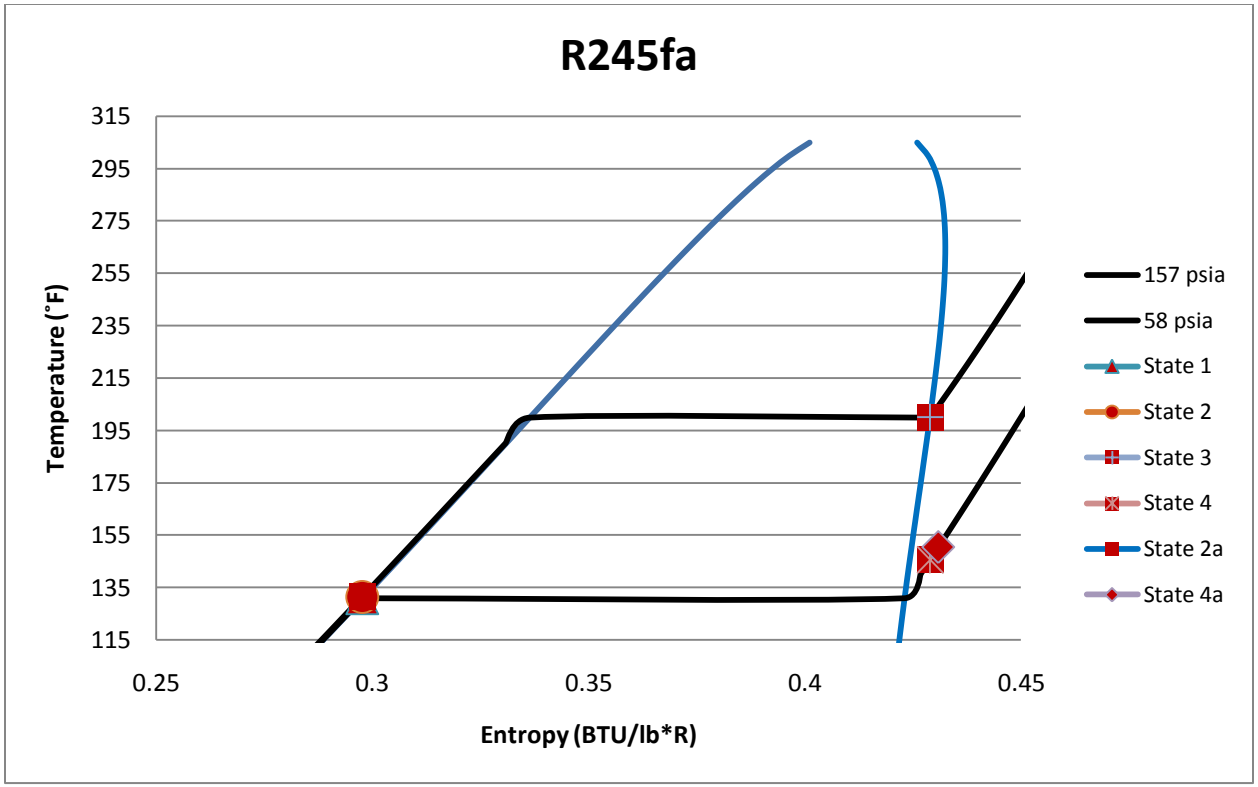
R245fa
315
295
275
255
235
215
195
175
155
135
115
Temperature (°F)
0.25
0.3
0.35
0.4
0.45
Entropy (BTU/lb*R)
157 psia
58 psia
State 1
State 2
State 3
State 4
State 2a
State 4a

Appendix B: ORC Matlab Code

```
7/5/11 8:45 AM \\tsclient\E\ORC_Thesis\Matlab\ORC_Rad.m 1 of 2
Azimuth = zeros(365,24); %azimuth angle
Altitude = zeros(365,24); %altitude angle
AirMass1 = zeros(365,24); %m (dimless)
AirMass = zeros(365,24); %m (dimless)
Ib = zeros(365,24); %Beam Rad (W/m^2)
Ibh = zeros(365,24); %Beam Horiz (W/m^2)
Idh = zeros(365,24); %Diffuse Horiz (W/m^2)
Ibc = zeros(365,24); %Beam Conc (W/m^2)
Idc = zeros(365,24); %Diffuse Conc (W/m^2)
Irc = zeros(365,24); %Reflect Conc (W/m^2)
Ic = zeros(365,24); %Total Rad on Conc (W/m^2)
N = zeros(365,1); %day number
Declination = zeros(365,1); %declination angle
hss = zeros(365,1); %Sunset hour angle
Io = zeros(365,1); %Extraterrestrial Radiation (W/m^2)
AppFlux = zeros(365,1); %Apparant Flux A (W/m^2)
OptDepth = zeros(365,1); %Optical Depth k (dimless)
C = zeros(365,1); %diffuse sky factor
Time = zeros(24,1); %time of day used as place holder
h = zeros(24,1); %Hour angle
A1 = zeros(24,1); %Constants used for comparison only
B1 = zeros(24,1); %Constants used for comparison only
Lat = 35.771667; %Latitude
Long = 78.638889; %Longitude
SolCons = 1.377; %SC (kW/m^2)
Rho = 0.2; %Ground reflectivity
for i = 1:365;
Declination(i) = 23.45*sind((360/365)*(284+i));
hss(i) = acosd(-tand(Lat)*tand(Declination(i)));
N(i) = i;
Io(i) = SolCons*1000*(1+0.034*cosd((360*N(i))/365));
AppFlux(i) = 1160+75*sind((360/365)*(N(i)-275));
OptDepth(i) = 0.174+0.035*sind((360/365)*(N(i)-100));
C(i) = 0.095+0.04*sind((365/360)*(N(i)-100));
for k = 1:24
Time(k) = k;
h(k) = (k-12)*15;
if h(k) >= -hss(i) && h(k) <= hss(i);
Altitude(i,k) = asind(sind(Lat)*sind(Declination(i))+cosd(Lat)*cosd
(Declination(i))*cosd(h(k)));
else
Altitude(i,k) = NaN;
end
A1(k) = cosd(h(k));
B1(k) = tand(Declination(i))/tand(Lat);
7/5/11 8:45 AM \\tsclient\E\ORC_Thesis\Matlab\ORC_Rad.m 2 of 2
if A1(k) < B1(k) && h(k) < 12;
Azimuth(i,k) = -180+abs(asind((cosd(Declination(i))*sind(h(k)))/cosd
```

```
(Altitude(i,k))));
elseif A1(k) < B1(k) && h(k) >= 12;
Azimuth(i,k) = 180-
asind((cosd(Declination(i))*sind(h(k)))/cosd(Altitude(i,
k)));
else
Azimuth(i,k) =
asind((cosd(Declination(i))*sind(h(k)))/cosd(Altitude(i,k)));
end
AirMass1(i,k) = 1/sind(Altitude(i,k));
if AirMass1(i,k) >= 7;
AirMass(i,k) = 7;
else AirMass(i,k) = AirMass1(i,k);
end
Ib(i,k) = AppFlux(i)*exp(-OptDepth(i)*AirMass(i,k));
Ibh(i,k) = Ib(i,k)*sind(Altitude(i,k));
Idh(i,k) = C(i)*Ib(i,k);
Ibc(i,k) = Ib(i,k)*cosd(Declination(i));
Idc(i,k) = Idh(i,k)*.5*(1-cosd(Lat));
Irc(i,k) = Rho*(Ibh(i,k)+Idh(i,k))*.5*(1-cosd(Lat));
Ic(i,k) = Ibc(i,k)+Idc(i,k)+Irc(i,k);
end
end
n = input('Day Number: ');
figure(1); surf(Time,N,Ic), xlabel('AST (Hours)'), ylabel('Day Number'),
zlabel
('Insolation on Collector (W/m^2)'), title('Insolation on Collector Vs.
Hours Vs.
Days');
figure(2); surf(Time,N,Ibc), xlabel('AST (Hours)'), ylabel('Day Number'),
zlabel('Beam
on Collector (W/m^2)'), title('Insolation on Collector Vs. Hours Vs.
Days');
figure(3); surf(Time,N,Idc), xlabel('AST (Hours)'), ylabel('Day Number'),
zlabel
('Diffuse on Collector (W/m^2)'), title('Insolation on Collector Vs. Hours
Vs. Days');
figure(4); surf(Time,N,Irc), xlabel('AST (Hours)'), ylabel('Day Number'),
zlabel
('Reflected on Collector (W/m^2)'), title('Insolation on Collector Vs.
Hours Vs. Days');
figure(5); plot(Time,Ic(n,1:24)), xlabel('AST (Hours)'),
ylabel('Insolation on Collector
(W/m^2)'), title('Insolation on Collector Vs. Hours for Day n');
```

Appendix C: Case Study Spreadsheet

Heat Flow out of baghouse exhaust

Q=m*Cp*dT

Assumptions

Aceton is main source of combustion
Average specific heat
Constant Density
Only Exhausts CO2 and H2O
Power output is heat transfer divided by 35000
Based on infinity turbine

Stoiciometric Equation

(CH3)2CO+4(O2+3.76N2) -> 3CO2+3H2O+15.04N2

This means that for every one part of fuel you need 4 parts of air

AF's	9.467586207	

Temperatures

Texhaust	365	^{o}F
THXoil	180	^{o}F

Specific Heat of Air

at 365	0.24429	BTU/lbm*F
at 200	0.2409	BTU/lbm*F
Average	0.242595	BTU/lbm*F

						28.08						
Desnisty of Acetone						44.35668						
Average	49.5	lbm/ft^3										
Fuel Flow rate												
Average	37	lbm/min								One Kiln		
										Assuming 300% Excess Air		
Stoichiometric Analysis			Lean Analysis (ϕ=.75)			Rich Analysis (ϕ=1.25)			Lean Analysis (ϕ=.33)			
Air Flow Rate			**Air Flow Rate**			**Air Flow Rate**			**Air Flow Rate**			
Average	21018.04138	lbm/hr	Average	11840	lbm/hr	Average	7104	lbm/hr	Average	84072.17	lbm/hr	
Heat Transfer			**Heat Transfer**			**Heat Transfer**			**Heat Transfer**			
Q dot	943291.2735	BTU/hr	Q dot	531380.1	BTU/hr	Q dot	318828.1	BTU/hr	Q dot	3773165	BTU/hr	
Power Output			**Power Output**			**Power Output**			**Power Output**			
P	26.95117924	kW	P	15.18229	kW	P	9.109373	kW	P	107.8047	kW	
If units were wrong and it is gal/min not lbm												
Fuel Flow rate												
Average	37	gal/min										
Average	244.8359375	lbm/min										

Stoichiometric Analysis			Lean Analysis (ϕ=.75)			Rich Analysis (ϕ=1.25)			Lean Analysis (ϕ=.33)		
Air Flow Rate			**Air Flow Rate**			**Air Flow Rate**			**Air Flow Rate**		
Average	58760.625	lbm/hr	Average	78347.5	lbm/hr	Average	47008.5	lbm/hr	Average	176281.9	lbm/hr
Heat Transfer			**Heat Transfer**			**Heat Transfer**			**Heat Transfer**		
Q dot	2637181.257	BTU/hr	Q dot	3516242	BTU/hr	Q dot	2109745	BTU/hr	Q dot	7911544	BTU/hr
Power Output			**Power Output**			**Power Output**			**Power Output**		
P	75.34803592	kW	P	100.464	kW	P	60.27843	kW	P	226.0441	kW

Loan Principal	$ 280,000	**Energy Savings (kWh/yr)**	1878240
Interest	0.08	**Price at t=0 ($/kWh)**	$ 0.0549
Loan Term (yr)	20	**Savings t=0 ($/yr)**	$ 103,115
CRF (1/yr)	0.101852209	**Escalating at (1/yr)**	0.05
Payments ($/yr)	$ 28,519		
Tax Bracket	0.305	**Personal Discount Rate**	0.10

End of Year	Loan Payment	Interest	Delta Principal	Loan Balance	Tax Savings	Loan Cost	Electric Savings	Net Savings	PV Savings	Cum Pv Savings
0	$0	$0	$0	$280,000	$0	$0	$0	$0	$0	$0
1	$28,519	$22,400	$6,119	$273,881	$6,832	$21,687	$108,271	$86,585	$78,713	$78,713
2	$28,519	$21,911	$6,608	$267,273	$6,683	$21,836	$113,685	$91,849	$75,908	$154,621
3	$28,519	$21,382	$7,137	$260,137	$6,521	$21,997	$119,369	$97,372	$73,157	$227,778
4	$28,519	$20,811	$7,708	$252,429	$6,347	$22,171	$125,337	$103,166	$70,464	$298,242
5	$28,519	$20,194	$8,324	$244,105	$6,159	$22,359	$131,604	$109,245	$67,832	$366,074
6	$28,519	$19,528	$8,990	$235,114	$5,956	$22,562	$138,184	$115,622	$65,266	$431,340
7	$28,519	$18,809	$9,709	$225,405	$5,737	$22,782	$145,094	$122,312	$62,765	$494,105
8	$28,519	$18,032	$10,486	$214,919	$5,500	$23,019	$152,348	$129,330	$60,333	$554,439
9	$28,519	$17,193	$11,325	$203,593	$5,244	$23,275	$159,966	$136,691	$57,970	$612,409
10	$28,519	$16,287	$12,231	$191,362	$4,968	$23,551	$167,964	$144,413	$55,678	$668,087
11	$28,519	$15,309	$13,210	$178,153	$4,669	$23,849	$176,362	$152,513	$53,455	$721,541
12	$28,519	$14,252	$14,266	$163,886	$4,347	$24,172	$185,180	$161,009	$51,302	$772,844
13	$28,519	$13,111	$15,408	$148,478	$3,999	$24,520	$194,439	$169,920	$49,220	$822,063
14	$28,519	$11,878	$16,640	$131,838	$3,623	$24,896	$204,161	$179,266	$47,206	$869,270
15	$28,519	$10,547	$17,972	$113,867	$3,217	$25,302	$214,369	$189,068	$45,261	$914,531
16	$28,519	$9,109	$19,409	$94,457	$2,778	$25,740	$225,088	$199,348	$43,384	$957,915
17	$28,519	$7,557	$20,962	$73,495	$2,305	$26,214	$236,342	$210,128	$41,573	$999,488
18	$28,519	$5,880	$22,639	$50,856	$1,793	$26,725	$248,159	$221,434	$39,827	$1,039,314
19	$28,519	$4,068	$24,450	$26,406	$1,241	$27,278	$260,567	$233,290	$38,145	$1,077,459
20	$28,519	$2,112	$26,406	$0	$644	$27,874	$273,596	$245,721	$36,525	$1,113,984

Assuming 250kW system

Cost	380000	$ (+)	
Fed Grant	114000	$ (-)	30% of total cost
Tax Cred	50000	$ (-)	10% of total cost, capped at 200$/kW
Subsidy	6,489	$ (-)	.6$/ft^2 if it makes a step toward cutting energy use in half
Duct	2000	$ (+)	125 ft of 8" and 25 ft of 6" Means
Concrete	1500	$ (+)	20'x10'x6" @ 70$/ton Means
R-245fa	18000	$ (+)	1500 lb @ 12$/lb
HX	10000	$ (+)	Airec Compact 70 Estimated
Tech	100	$ (+)	20 $/hr @ 5 hr
Pump	21300	$ (+)	1 for hot water 1 for cold water Assumed from Means
Water Tank	10000	$ (+)	2000 gal estimated from means
Shipping	5000	$ (+)	From UPS Freight Website
Total	**$ 277,411.00**		

Elec Gen	103115.376	$/yr (-)	
Pump Work	7194.096	$ (+)	Electrical usage for 3 pumps

Payback	**34.7048**	**Months**
	2.8921	**Year**

n	Elec price	Elec Gen	Pump work	Payback (yr)
1	0.055	103115.376	7194.096	2.892
2	0.058	108271.145	7553.801	2.754
3	0.061	113684.702	7931.491	2.623
4	0.064	119368.937	8328.065	2.498
5	0.067	125337.384	8744.469	2.379
6	0.070	131604.253	9181.692	2.266
7	0.074	138184.466	9640.777	2.158
8	0.077	145093.689	10122.816	2.055
9	0.081	152348.374	10628.956	1.957
10	0.085	159965.792	11160.404	1.864
11	0.089	167964.082	11718.424	1.775
12	0.094	176362.286	12304.346	1.691
13	0.099	185180.400	12919.563	1.610
14	0.104	194439.420	13565.541	1.534
15	0.109	204161.391	14243.818	1.461
16	0.114	214369.461	14956.009	1.391
17	0.120	225087.934	15703.809	1.325
18	0.126	236342.331	16489.000	1.262
19	0.132	248159.447	17313.450	1.202
20	0.139	260567.420	18179.122	1.144
21	0.146	273595.791	19088.078	1.090
22	0.153	287275.580	20042.482	1.038
23	0.161	301639.359	21044.606	0.989
24	0.169	316721.327	22096.837	0.942
25	0.177	332557.393	23201.679	0.897